Inelastic Scattering of 17-MeV Protons from Be^9, B^{10}, Ne^{20}, Mg^{25}, and Mg^{26}*

G. SCHRANK, E. K. WARBURTON,† AND W. W. DAEHNICK
Palmer Physical Laboratory, Princeton University, Princeton, New Jersey

(Received May 11, 1962)

Elastic and inelastic scattering of 17-MeV (center-of-mass energy) protons by Be^9, B^{10}, Ne^{20}, Mg^{25}, and Mg^{26} was studied using scintillation crystal spectroscopy. Angular distributions were obtained for most of the levels observed. All the angular distributions are characteristic of a direct interaction with initial- and final-state interactions. The differential cross sections were summed to obtain total cross sections which were compared to *EL* transition rates when known. For the larger (p,p') cross sections a strong correlation with the *EL* transition rates was found. This correlation is discussed in some detail.

I. INTRODUCTION

COLLECTED in this report are the results of the inelastic scattering of 17-MeV (approximate center-of-mass energy) protons by Be^9, B^{10}, Ne^{20}, Mg^{25}, and Mg^{26}. These results were obtained over a span of several years using the Princeton FM cyclotron. The results for Ne^{20} and Mg^{25} have been reported previously in abstract form.[1] Studies of the inelastic scattering of protons by light nuclei have been made previously at this laboratory for the lithium isotopes,[2] C^{12},[3] N^{14},[4] O^{16},[5] and Mg^{24}.[6,7] The present results, together with these previous results, constitute a rather broad albeit nondetailed survey of the inelastic scattering of 17-MeV protons by light nuclei. For instance, the only p-shell nuclei available as targets which have not been investigated at this laboratory are B^{11}, C^{13}, C^{14}, and N^{15}.

The purpose of this inelastic scattering work was twofold: first, to investigate the reaction mechanism; and second, to see to what extent the (p,p') reaction could be used as a tool in nuclear spectroscopy. It has been known for several years that for proton energies less than about 10 MeV the (p,p') reaction in the light nuclei proceeds by a mixture of compound nucleus formation and the direct interaction mechanism. In the range $10<E_p<16$ MeV the relative contribution of compound nucleus formation diminishes rapidly,[8] and although the evidence is meager, it is expected that the effects of compound nucleus resonances are not too important above this proton energy range. Proton inelastic scattering from light nuclei in the energy range $16<E_p<30$ MeV has not been reported by other laboratories.

The first attempts to obtain a theoretical expression for the (p,p') direct interaction were in terms of a zero range, plane wave Born approximation. This leads to the result[9,10]

$$\sigma(\theta)=(k_f/k_i)\sum_L A_L(n_f l_f|\, j_L(qr)\,|n_i l_i)^2, \qquad (1)$$

where the A_L contain all the information of spectroscopic interest. The wave vectors $\mathbf{k}_i$ and $\mathbf{k}_f$ are for the incident and scattered protons, q is the momentum transfer $\mathbf{q}=\mathbf{k}_i-\mathbf{k}_f$, $j_L(qr)$ is a spherical Bessel function of order L, nl represents the one-particle quantum numbers of a bound nucleon, and $(n_f l_f|\, j_L(qr)\,|n_i l_i)$ is the expectation value of $j_L(qr)$ over the radial wave function of the particle making the transition. The sum over L is restricted by various selection rules, some of which are model dependent. If the reaction is assumed to be limited to the nuclear surface then $(n_f l_f|\, j_L(qr)\,|n_i l_i)$ is replaced by $j_L(qR)$, where R is the nuclear radius. This is the surface interaction result first given by Austern, Butler, and McManus.[11] Another approach[10] is to use harmonic oscillator wave functions and obtain $(n_f l_f|\, j_L(qr)\,|n_i l_i)$ by integration over all space.

As an example of the plane wave theory both of these forms of Eq. (1) are shown in Fig. 1 for the case of the $Be^9(p,p')Be^9$ (2.43-MeV level) reaction. The experimental points were taken at a proton energy of 31.3 MeV by Benveniste, Finke, and Martinelli.[12] Both theoretical curves in Fig. 1 are for $L=2$ as is predicted by the shell model.[13] It is conjectured by Levinson and Banerjee[10] that for the lightest nuclei the nuclear surface is so ill defined that the volume integration evaluation of $(n_f l_f|\, j_L(qr)\,|n_i l_i)$ should be the more appropriate approximation to make. This point is supported by the experimental results shown in Fig. 1 which give no evidence of the secondary maximum which is predicted by $j_2^2(qR)$.

The most noticeable result of the (p,p') work done at this laboratory is the almost complete failure of the

* This work was supported by the U. S. Atomic Energy Commission and the Higgins Scientific Trust Fund.

† Present address: Brookhaven National Laboratory, Upton, New York.

[1] G. Schrank and G. K. O'Neill, Bull. Am. Phys. Soc. **1**, 29 (1956); G. Schrank and E. K. Warburton, *ibid.* **4**, 220 (1959).

[2] Li^6: R. Sherr and W. F. Hornyak; Li^7: D. R. Maxson and E. Bennett, both reported by C. A. Levinson and M. K. Banerjee, Ann. Phys. (New York) **2**, 471 (1957).

[3] R. W. Peelle, Phys. Rev. **105**, 1311 (1957).

[4] W. Daehnick (to be published).

[5] W. F. Hornyak and R. Sherr, Phys. Rev. **100**, 1409 (1955).

[6] P. C. Gugelot and P. R. Phillips, Phys. Rev. **101**, 1613 (1956).

[7] W. Daehnick (to be published).

[8] See, for instance, *Proceedings of the International Conference on Nuclear Structure*, edited by D. A. Bromley and E. W. Vogt (University of Toronto Press, Toronto, 1960), pp. 163–164, 223–225.

[9] C. A. Levinson in *Nuclear Spectroscopy*, edited by F. Ajzenberg-Selove (Academic Press Inc., New York, 1960), Part B, p. 670.

[10] C. A. Levinson and M. K. Banerjee, Ann. Phys. (New York) **2**, 471 (1957); **2**, 499 (1957); **3**, 67 (1958).

[11] N. Austern, S. T. Butler, and H. McManus, Phys. Rev. **92**, 350 (1953).

[12] J. Benveniste, R. G. Finke, and E. A. Martinelli, Phys. Rev. **101**, 655 (1956).

[13] W. T. Pinkston, Phys. Rev. **115**, 963 (1959).

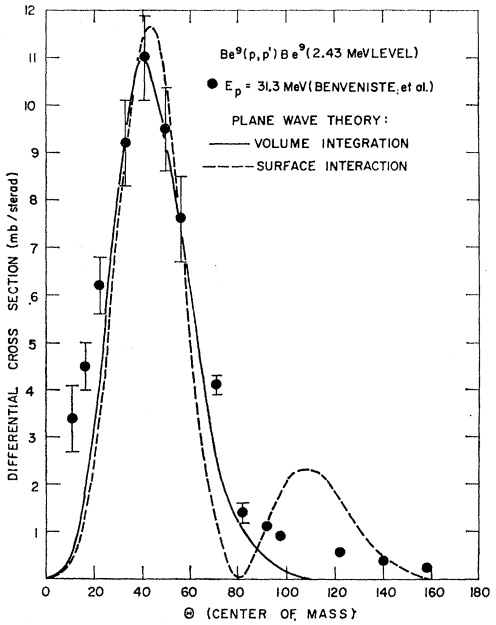

FIG. 1. Comparison of the (p,p') plane-wave, zero-range Born approximation with the experimental data of Benveniste, Finke, and Martinelli (reference 12) for the $Be^9(p,p')Be^9$(2.43-MeV level) reaction. The theoretical curves are arbitrarily normalized to the experimental data. The volume integration was done using an oscillator well parameter b_p equal to 2.6 F (see reference 2), the surface interaction is for a nuclear radius of 4.15 F.

plane wave theory to explain the observed proton angular distributions. In fact, the $Li^6(p,p')Li^6$ (2.19-MeV level) reaction[2] which was observed for $E_p=14.8$ and 19.4 MeV is the only light nucleus reaction for which the plane wave theory prediction remotely resembles the experimental angular distributions obtained at this laboratory. In recent years the major theoretical emphasis on the proton direct interaction has been to develop a distorted wave, finite range theory which would explain these and other results. This was first done by Levinson and Banerjee[10] who had considerable success in fitting the extensive experimental results for the $C^{12}(p,p')C^{12}$ (4.43-MeV level) reaction. As an example of the effects of distortion, angular distribution results taken at proton energies of 12,[14] 31.3,[12] and 18.9 MeV for the $Be^9(p,p')Be^9$ (2.43-MeV level) reaction are shown in Fig. 2. The 18.9-MeV results are from the present work (see Sec. IIIA). In Fig. 2 the momentum transfer q in units of 10^{13} cm^{-1} is shown plotted against the differential cross section multiplied by k_i/k_f. If the plane wave theory given by Eq. (1) were valid then the experimental points in Fig. 2 would lie on a universal curve independent of proton energy.

As is evident from Fig. 1, the 31.3-MeV results are in rather good agreement with the plane wave theory. The 18.9- and 12-MeV results, however, show little resemblance to the plane wave theory as is evident from the comparison of Fig. 2. These results are typical of the angular distributions for light nuclei observed at this laboratory. At both energies the maxima associated with the plane wave theory do not appear and there is a large preponderance of protons scattered in the forward direction. This is just the sort of behavior that Levinson and Banerjee[10] found the distorted wave theory could explain in the case of the $C^{12}(p,p')C^{12}$ (4.43-MeV level) reaction. An examination of Fig. 2 shows that the total cross section is rising more rapidly with decreasing proton energy than is predicted by the plane wave theory. This is also true of the C^{12} 4.43-MeV level cross section in this same proton energy range, and again can be explained by the distorted wave theory.[10]

Later theoretical work[15,16] using one form or another of the distorted wave theory has met with partial success in explaining (p,p') angular distributions for light nuclei in the energy range of 17 to 20 MeV, and it would seem that one of these forms would be capable of explaining the present work. For this reason the experimental results are given in tabular form so that they will be most easily available for comparison with later theoretical work.

A striking feature of inelastic scattering is that the relative cross sections for the excitation of various levels in a given nucleus are remarkably constant as a function of bombarding energy and practically independent of the type of bombarding particle. This is illustrated by the case of Be^9. Summers-Gill[14] studied the inelastic scattering of 12-MeV protons, 24-MeV

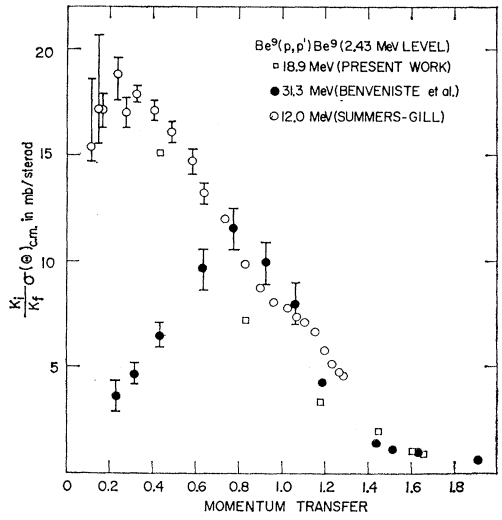

FIG. 2. Comparison of the $Be^9(p,p')Be^9$(2.43-MeV level) reaction at three proton energies, 12 MeV (reference 14), 18.9 MeV (present work), and 31.3 MeV (reference 12). The momentum transfer q is in units of 10^{13} cm^{-1}. If the plane-wave, zero-range Born approximation of Eq. (1) were correct then the experimental points would lie on a universal curve.

[14] R. G. Summers-Gill, Phys. Rev. **109**, 1591 (1958).

[15] N. K. Glendenning, Phys. Rev. **114**, 1297 (1959).

[16] E. S. Rost, University of Pittsburgh thesis, 1961 (unpublished), and references therein.

deuterons, and 48-MeV α particles from Be^9 and found quite similar spectra in the three cases. The 2.43-MeV level and a level near 6.8 MeV were excited strongly in all these reactions while the other levels were not. The $Be^9(p,p')Be^9$ reaction has been studied at a proton energy of 185 MeV[17] as well as at the energies shown in Fig. 2. In all these studies the relative cross sections are the same within the experimental errors.

Two conclusions are suggested by these two features of inelastic scattering. The first is that distortion effects are quite nearly the same for different low-lying levels of the same nucleus. The second is that the spin-dependent part of the nucleon-nucleon interaction is contributing a relatively small amount to the cross section in (p,p') and (d,d') reactions. These two conclusions are supported and qualitatively explained by recent studies of the inelastic scattering. Cohen and Rubin[18] found a significant correlation between the cross sections for inelastic proton scattering and for Coulomb excitation. This was predicted theoretically by Bohr.[19] Pinkston and Satchler[20] examined the analogy between nuclear excitation, on a plane-wave direct-interaction model, and electric multipole radiation. They concluded that if an EL transition between two states is enhanced by collective effects, the inelastic scattering will be also; but, that the spin-dependent transitions are not enhanced when the spin-independent transitions are. Rost[16] examined the relationship between the EL transition and inelastic scattering in a detailed, distorted-wave treatment of the $Mg^{24}(p,p')Mg^{24}$ (1.37-MeV level) reaction. He found that the relationship holds independently of distortion. That is, to a good approximation, collective enhancement leads to an over-all multiplicative factor for the differential cross section calculated from a spin-independent nucleon-nucleon interaction.

These considerations lead us to expect that the strong inelastic transitions will be those for which the EL transition is enhanced, and for these transitions the contribution of the spin-dependent matrix elements will usually be negligible so that the cross sections will be proportional to the EL transition rates. If then, the distortion changes little with excitation energy as is indicated, the L-wave (p,p') cross sections for a given nucleus will be proportional to the EL transition rates to the ground state at least for the strong transitions. In Sec. III the present results are examined to see to what extent this proportionality holds. In order to do this, the differential cross sections were integrated to obtain total cross sections for each level. By comparing total cross sections it is hoped that uncertainties due to the angular dependence of the distortion will be minimized. In Sec. IV a comparison is made between $E2$ transition rates and $L=2$ (p,p') total cross sections for some low-energy $E2$ ground-state transitions in various nuclei in the p shell and (s,d) shells.

II. EXPERIMENTAL PROCEDURE

Various thin targets were bombarded with the external beam of protons from the Princeton FM cyclotron. The 60-in. scattering chamber, previously described by Yntema and White[21] was used in these experiments. Details of the beam current monitor, geometrical arrangement, counting rates, etc., are given in previous work.[22] The bombarding energy was measured to an accuracy of ± 0.1 MeV and regulated to ± 20 keV by means of a "proton range to cyclotron magnet" feedback system.[23] The proton bombarding energy spread was about 200 keV.

The reaction particles were detected with thin NaI(Tl) crystal spectrometers. The resolution of the various spectrometers was between 2 and 3% full width at half-maximum for 17-MeV protons. The data were collected with a multi-channel analyzer. The data analysis was greatly facilitated by an IBM 650 computer program which yielded the conversion factors for transformation of scattering angles and differential cross sections to the center-of-mass system and gave the scattered proton energies at 5-deg intervals.[24]

III. RESULTS

A. Be^9

Experimental Results

The Be^9 target consisted of a 0.005-in. thick Be^9 foil which contained negligible oxygen and carbon contamination. The laboratory bombarding energy was 18.9 MeV. This energy corresponds to 17 MeV in the center-of-mass system and is the energy at which Dayton and Schrank[22] had previously measured the differential cross section for the elastic scattering of protons by twelve elements, including Be^9, at 5 deg intervals from 15 to 172 deg and with an accuracy of 2.5% or better. Thus, the differential cross sections for the inelastic proton groups could be determined at each angle from a comparison of the intensities of the inelastic groups with that of the $Be^9(p,p)Be^9$ elastic group.

A pulse-height spectrum of the scattered particles observed at 60° to the bombarding proton beam is shown in Fig. 3. The deuteron peak due to the $Be^9(p,d)Be^8$ ground-state reaction ($Q=0.560$ MeV) and the proton peak corresponding to the Be^9 2.43-MeV level are easily discernible. The background is mainly due to the three-body process, $Be^9(p,pn)Be^8$, which

[17] H. Tyrén and Th. A. J. Maris, Nuclear Phys. **6**, 82 (1958).
[18] B. L. Cohen and A. G. Rubin, Phys. Rev. **111**, 1568 (1958).
[19] A. Bohr, Physica **22**, 963 (1956).
[20] W. T. Pinkston and G. R. Satchler, Nuclear Phys. **27**, 270 (1961).
[21] J. L. Yntema and M. G. White, Phys. Rev. **95**, 1226 (1954).
[22] I. E. Dayton and G. Schrank, Phys. Rev. **101**, 1358 (1956).
[23] G. Schrank, Rev. Sci. Instr. **26**, 677 (1955).
[24] We are indebted to J. Christenson who wrote the 650 program and applied it to our transformations.

TABLE I. Experimental results for $Be^9(p,p')Be^{9*}$ in the laboratory and center-of-mass systems. The angles are in degrees and the differential cross sections in mb/sr.

		Excitation energy (MeV)								
		2.43			3.04			6.76		
θ(lab)	θ(c.m.)[a]	$\sigma(\theta)_{lab}$	Δ(%)	$\sigma(\theta)_{c.m.}$	$\sigma(\theta)_{lab}$	Δ(%)	$\sigma(\theta)_{c.m.}$	$\sigma(\theta)_{lab}$	Δ(%)	$\sigma(\theta)_{c.m.}$
30	33.4	17.0	2.4	14.0	2.5	50	2.0	2.0	50	1.6
60	66.0	7.5	2.7	6.7	0.6	33	0.5	2.2	33	1.9
90	97.0	3.15	4.8	3.17	0.8	25	0.8	1.0	50	1.0
120	126.0	1.6	6.2	1.82	0.3	67	0.35	<1.0	...	<1.2
150	153.4	0.8	12.5	1.00	<0.5	...	<0.60	<1.0	...	<1.3
170	171.2	0.68	12.0	0.87	<0.5	...	<0.65	<1.0	...	<1.4

[a] For the 2.43-MeV level. For the 6.76-MeV level θ(c.m.) =98.3° at θ(lab) =90°.

has a Q value of -1.667 MeV. The proton peaks due to the 3.04-MeV level and the broad 6.76-MeV level can also be seen rising above the background.

Spectra were taken at 30°, 60°, and 90° with a 0.027-in. aluminum foil in front of the NaI(Tl) crystal in order to remove the deuterons and any tritons or alpha particles which may have been present. In these spectra the presence of a broad proton peak corresponding to the 4.74-MeV level of Be^9 was apparent. The width of the proton peak was consistent with the width of 1.25 MeV reported for this level.[25] In Fig. 3 the proton peak due to this level is obscured by the deuteron peak corresponding to the broad Be^8 2.9-MeV level.

The experimental results for Be^9 are summarized in Table I. The excitation energies of the levels are taken from the literature.[25] The cross section for the 4.74-MeV level could not be obtained with any accuracy; however, it appears to be of the order of 1 mb/sr at the forward angles with a total cross section, within a factor of 3, of 4 mb. The width of the 6.76-MeV level was estimated by subtracting the assumed background indicated by the dashed curve in Fig. 3. The result is shown by the open circles which are fitted quite well by a Gaussian curve with a full width at half-maximum of 1.37 MeV in the laboratory system. By correcting this width for the 2.3% resolution, a center-of-mass width for the Be^9 6.76-MeV level of 1.2 ± 0.3 MeV is obtained.

The Be^9 levels indicated in Fig. 3 are the only ones known below 7-MeV excitation with the exception of the "level" at 1.75 MeV. A level near this energy was not seen in the present work. An upper limit for its cross section of 1/50th that of the 2.43-MeV level can be placed for each angle of observation.

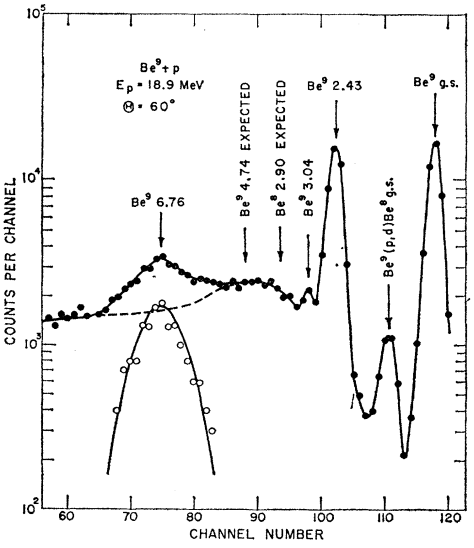

FIG. 3. Pulse-height spectrum of Be^9+p observed at 60° to the proton beam at a proton energy of 18.9 MeV. The peaks are labeled by the isotope and excitation energy to which they are assumed to belong. The dashed curve shows the assumed course of the background under the Be^9 6.76-MeV level group. The open circles are the difference between the experimental points and the dashed curve. A Gaussian curve has been fitted to the open circles.

Discussion

The level scheme of Be^9 is shown in Fig. 4 which is based on the compilation of Ajzenberg-Selove and Lauritsen[25] with later information from the work of Spencer, Phillips, and Young,[26] of Jakobson,[27] and of Blair.[28] According to Spencer *et al.*,[26] the 1.75-MeV level is "not a state in the usual sense of representing an energy situation of Be^9 which is unusually stable due to attractive forces" but is "an aspect of spatial localization of s-wave nucleons due to the two-body nature of nuclear states."

The spin-parity assignments to the 3.04- and 4.74-MeV levels are from the $Be^9(\gamma,n)Be^8$ work of Jakobson.[27] The assignment for the 3.04-MeV level is supported by the work of Spencer *et al.*[26] If the scheme of Fig. 4 is correct there is no evidence for the $1/2^-$ state of Be^9 which is predicted below 4 MeV by intermediate-coupling calculations.[29] However, this state could easily be obscured by the 3.04-MeV level which has a width of 250 ± 50 keV.[26]

[25] F. Ajzenberg-Selove and T. Lauritsen, Nuclear Phys. **11**, 1 (1959).

[26] R. R. Spencer, G. C. Phillips, and T. E. Young, Nuclear Phys. **21**, 310 (1960).

[27] M. J. Jakobson, Phys. Rev. **123**, 229 (1961).

[28] J. S. Blair, Phys. Rev. **123**, 2151 (1961).

[29] D. Kurath, Phys. Rev. **101**, 216 (1956).

The states observed in the present work and the total (p,p') cross sections are indicated in Fig. 4. The relative intensities with which the various levels are excited are in qualitative agreement with other (p,p') work[12,14] and with results for the inelastic scattering of deuterons and α particles.[14,30] As discussed in Sec. I, the similarity of the (p,p'), (d,d'), and (α,α') results supports the contention that the spin-dependent part of the nucleon-nucleon interaction contributes a relatively small amount to the total cross section.

Inelastic scattering from Be^9 has been considered by Blair and Henley[31] and by Kunz[32] using an α-particle model for Be^9, and by Pinkston[13] using the shell model with intermediate coupling. These three calculations are in rather good agreement, indicating that the two models give alternate descriptions of Be^9. The α-particle model is essentially the rotational model. In both calculations the spin dependence of the nucleon-nucleon interaction is neglected. The two calculations predict that the lowest $5/2^-$ and $7/2^-$ states of Be^9 are the only negative parity states below 9 MeV in Be^9 which can be excited to any appreciable extent by inelastic scattering. This can be understood most easily from the viewpoint of the rotational model which classifies the $3/2^-$ ground state and the $5/2^-$ and $7/2^-$ states as members of the $K=3/2$ band. Then (p,p') transitions for which $\Delta K \neq 0$ are inhibited because they are not collectively enhanced. Since their excitation energies and inelastic scattering cross sections are consistent with theoretical predictions,[29,13] it is suggested[12,31,32] that the Be^9 2.43- and 6.76-MeV levels are the $5/2^-$ and $7/2^-$ states, respectively. If so, the ratio of the 6.76-MeV level cross section to that of the 2.43-MeV level, 0.24 ± 0.15, is in fair agreement with the shell-model plane-wave prediction of Pinkston[13] which gives 0.35 as the ratio neglecting kinematical factors, but is somewhat lower than the rotational model predictions of ~ 0.5. It should be pointed out that the (p,p') cross sections are expected to be very insensitive to excitation energy. In the plane-wave theory the (p,p') cross section has negligible dependence on $E_x(=-Q)$ for small enough E_x ($E_x<8$ MeV for 17-MeV protons), and it does not seem likely that the distortion will vary appreciably with E_x. The largest effect is probably that of the Coulomb barrier which might give $\sim 20\%$ effect on the Be^9 6.76-MeV level cross section relative to that of the 2.43-MeV level. In the remainder of this section and in the next section the dependence of the cross section on E_x will be neglected.

If the Be^9 2.43-MeV level is $5/2^-$ then the shell-model theory predicts that the $Be^9(p,p')Be^9$ (2.43-MeV level) should correspond to $L=2$ while the α-particle model predicts contributions from both $L=2$ and $L=4$.[31,32] The $Be^9(p,p')Be^9$ (2.43-MeV level) data of Beneveniste *et al.* were originally fitted on the plane-wave theory with $L=1$.[12] The fit shown in Fig. 1 illustrates that the plane wave theory with $L=2$ supplies an equally acceptable fit to the data. Therefore, the (p,p') angular distribution at 31.3-MeV as well as all the relative inelastic cross section data support an assignment of $5/2^-$ to the Be^9 2.43-MeV level.

The excitation of single-particle states, i.e., $p^4 2s$ and $p^4 1d$, is predicted by both the collective model[31] and the shell model.[13] The Be^9 1.75-, 3.04-, and 4.74-MeV levels are candidates for single-particle states; and, if the spin-parity assignments of Fig. 4 are correct, these states are expected to belong predominantly to the $p^4 2s$ and $p^4 1d$ configurations. We would expect that the 1.75-MeV level was mostly $(p^4)_{J=0}+2s_{1/2}$ while the work of Blair indicates that the 3.04-MeV level is largely $(p^4)_{J=0}+1d_{5/2}$. Pinkston predicted the cross sections for the excitation of $(p^4)_{J=0}+2s_{1/2}$ and $(p^4)_{J=0}+1d_{5/2}$ relative to that of the p^5, 5/2 state in extreme jj coupling. The predicted cross sections were quite large. The small relative cross sections observed for the even-parity states of Be^9 in the present work and in other inelastic scattering investigations are probably due to two factors: The wave functions of these states are not well described by extreme jj coupling, and as is expected on the rotational model, there is considerably more collective enhancement of the $3/2^- \rightarrow 5/2^-$ transition than of the $3/2^- \rightarrow 1/2^+$ and $3/2^- \rightarrow 5/2^+$ transitions. The very small transition to the 1.75-MeV level supports the viewpoint that it is not a "normal" state.[25,26]

B. B^{10}

Experimental Results

The B^{10} target consisted of boron powder, enriched to 96% in B^{10}, suspended in a thin film of polystyrene

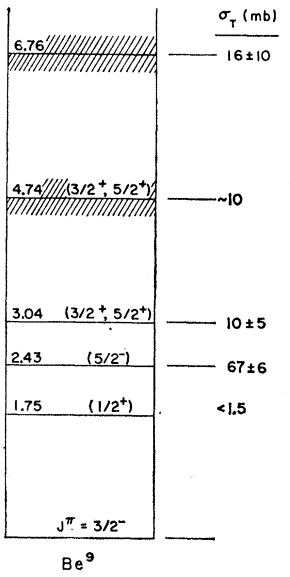

FIG. 4. Energy levels of Be^9. The spin-parity assignments are from references 25, 26, and 28. The levels observed in the present work and the total (p,p') cross sections for these levels are indicated.

[30] G. W. Farwell and A. I. Yavin, Cyclotron Research, University of Washington, Annual Progress Report, 1957 (unpublished).
[31] J. S. Blair and E. M. Henley, Phys. Rev. **112**, 2029 (1959).
[32] P. D. Kunz, Ann. Phys. (New York) **11**, 275 (1960).

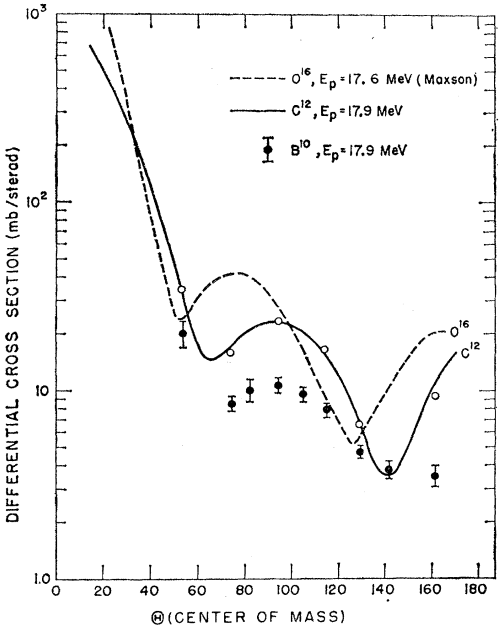

FIG. 5. Elastic scattering angular distributions for O^{16}, C^{12}, and B^{10}. The O^{16} curve is from reference 34. For C^{12}, the open circles illustrate the normalization of the present data to previous work of Daehnick and Sherr (reference 33) which is given by the full line. The $B^{10}(p,p)B^{10}$ angular distribution is from the present work.

$(CH)_n$. The ratio of the number of B^{10} atoms to C^{12} atoms in the target was measured by comparing the relative intensities of the B^{10} and C^{12} elastic peaks at backward angles with the relative intensities of these peaks obtained using a B_4C target. The B_4C target, which contained natural boron (18.8% B^{10}), was made by suspending a slurry of finely powdered B_4C in water on a 0.00025-in. platinum foil. The result was 2.2 ± 0.2 for the ratio of B^{10} to C^{12} atoms in the B^{10} target. This result was checked by dissolving the polystyrene after the experiment was finished. This method yielded 2.4 ± 0.2 for the ratio of B^{10} atoms to C^{12} atoms. A value of 2.3 ± 0.2 was adopted. The bombarding energy was 17.95 MeV, corresponding to 16.35 MeV in the center-of-mass system. The target thickness was about 25 keV.

The presence of appreciable O^{16} contamination was apparent from the presence of the O^{16} elastic peak at backward angles. Other contaminants, including the 4% B^{11}, were not apparent. The elastic peaks were separated sufficiently for angles greater than 50° so that the intensities of the peaks could be obtained. In Fig. 5 is shown the angular distributions of the B^{10}, C^{12}, and O^{16} ground state scattering. The angular distributions of the B^{10} and C^{12} elastic peaks obtained in the present work are shown by the experimental points. The relative number of counts at the various angles were obtained for the B^{10} and C^{12} elastic peaks from the integrated proton beam which was checked by a monitor placed at $\theta=10°$. The C^{12} data (open circles in Fig. 5) were normalized to a previous determination[33] of the $C^{12}(p,p)C^{12}$ angular distribution (full line in Fig. 5) at 17.9 MeV. The normalization factor and the ratio of B^{10} to C^{12} atoms of 2.3 ± 0.2 was then used to obtain the $B^{10}(p,p)B^{10}$ absolute cross section. The results for $B^{10}(p,p)B^{10}$ are given in Table II. The B^{10} cross-section scale in Fig. 5 and the cross sections given in Table II have an estimated uncertainty of 15% in addition to the relative errors which are given. This uncertainty in the absolute scale is due to inexact knowledge of the integrated charge, target thickness, and solid angle subtended by the detector.

TABLE II. Experimental results for the elastic scattering of 17.9-MeV protons by B^{10}. The angles are in degrees and the cross sections are in mb/sr.

θ(lab)	$\sigma(\theta)_{lab}$	θ(c.m.)	$\sigma(\theta)_{c.m.}$	Δ(%)
50	22.6	54.4	20.0	17
70	9.1	75.4	8.5	9
80	10.3	85.7	10.0	15
90	10.8	95.8	10.8	11
100	9.2	105.7	9.6	9
110	7.3	115.4	7.9	9
125	4.2	129.7	4.7	8
140	3.2	143.7	3.8	11
160	2.9	162.0	3.5	14

The $O^{16}(p,p)O^{16}$ angular distribution at $E_p=17.6$ MeV was taken from previous work at this laboratory.[34] An excitation curve taken[35] at $\theta_{lab}=160°$ shows the 160° $O^{16}(p,p)O^{16}$ cross section to be flat to 5% from 17.4 to 18.1 MeV. Thus, the $O^{16}(p,p)O^{16}$ cross section at 17.9 MeV and $\theta_{lab}=160°$ is known as is the $C^{12}(p,p)C^{12}$ cross section and the O^{16} contamination in the target could be obtained from the relative intensities of the C^{12} and O^{16} elastic peaks at this angle. The

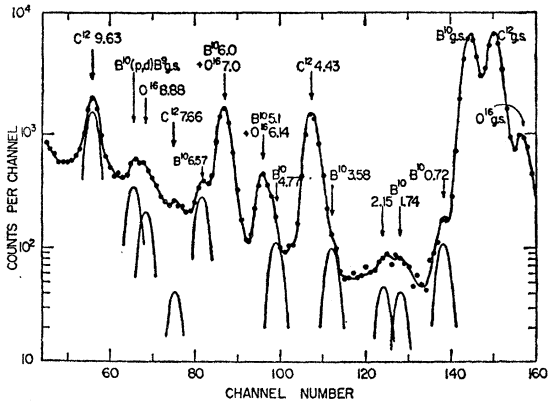

FIG. 6. Pulse-height spectrum of $B^{10}+p$ observed at 90° to the proton beam at a proton energy of 17.9 MeV. The peaks are labeled by the isotope and excitation energy to which they are assumed to belong. The Gaussian curves indicate the assumed shapes and intensities of unresolved peaks.

[33] W. Daehnick and R. Sherr (to be published). These data have an uncertainty of about 3% and are preferred over the earlier data of Peelle (reference 3) with which they disagree slightly.
[34] D. R. Maxson, Phys. Rev. **123**, 1304 (1961).
[35] R. Sherr and J. Christenson (unpublished).

TABLE III. Experimental results for $B^{10}(p,p')B^{10*}$ in the laboratory and center-of-mass systems. The angles are in degrees and the differential cross sections in mb/sr.

		Excitation energy (MeV)											
		0.72			1.74			2.15			3.58		
θ(lab)	θ(c.m.)[a]	$\sigma(\theta)_{lab}$	Δ(%)	$\sigma(\theta)_{c.m.}$	$\sigma(\theta)_{lab}$	Δ(%)	$\sigma(\theta)_{c.m.}$	$\sigma(\theta)_{lab}$	Δ(%)	$\sigma(\theta)_{c.m.}$	$\sigma(\theta)_{lab}$	Δ(%)	$\sigma(\theta)_{c.m.}$
20	22.1	5.5	30	4.5	...	...	...	...	...	...	1.0	25	0.8
28	30.8	4.0	30	3.4	0.18	70	0.15	0.57	35	0.48	...	...	...
30	33.0	2.8	25	2.4	...	...	...	0.77	25	0.65	...	...	...
50	54.7	0.64	50	0.57	0.09	50	0.08	0.32	15	0.28	0.57	10	0.49
70	75.7	0.22	25	0.21	0.11	25	0.10	0.12	20	0.11	0.32	15	0.30
90	96.1	0.11	40	0.11	0.08	50	0.08	0.07	40	0.07	0.12	40	0.12
100	106.0	0.15	50	0.16	0.07	25	0.07	0.08	20	0.09	...	...	...
110	115.7	0.13	30	0.14	0.07	30	0.07	0.12	25	0.13	...	...	...
125	130.0	0.16	25	0.18	0.07	50	0.08	0.09	50	0.11	...	...	...
140	143.9	...	...	...	0.03	30	0.04	0.06	30	0.07	...	...	...
160	162.1	0.20	20	0.24	0.06	25	0.07	0.10	25	0.12	...	...	...

		Excitation energy (MeV)											
		4.77			5.14±0.06			6.04±0.05			6.57		
θ(lab)	σ(c.m.)[a]	$\sigma(\theta)_{lab}$	Δ(%)	$\sigma(\theta)_{c.m.}$	$\sigma(\theta)_{lab}$	Δ(%)	$\sigma(\theta)_{c.m.}$	$\sigma(\theta)_{lab}$	Δ(%)	$\sigma(\theta)_{c.m.}$	$\sigma(\theta)_{lab}$	Δ(%)	$\sigma(\theta)_{c.m.}$
20	22.4	...	...	...	...	...	...	5.05	9	4.00	...	...	...
28	31.3	0.53	30	0.43	0.80	10	0.65	4.68	6	3.80	0.53	50	0.4
30	33.6	...	...	...	...	...	...	4.25	6	3.45	...	...	...
50	55.3	0.23	50	0.2	0.51	15	0.44	3.15	4	2.70	0.60	20	0.52
70	76.5	0.22	50	0.2	0.32	25	0.30	2.24	6	2.06	0.47	25	0.43
90	97.0	0.15	40	0.15	0.30	30	0.30	1.96	5.5	1.96	0.36	25	0.36
100	106.9	...	...	...	0.25	30	0.26	1.70	5	1.80	0.28	40	0.3
110	116.5	...	...	...	0.30	25	0.33	2.12	4.5	2.34	0.18	50	0.2
125	130.7	...	...	...	0.22	15	0.26	1.80	7	2.10	0.17	50	0.2
140	144.5	0.12	50	0.15	0.18	20	0.22	1.50	19	1.83	...	...	...
160	162.4	0.10	50	0.13	0.19	15	0.24	1.27	13	1.64	0.07	50	0.1

[a] Mean value for the four levels ±0.4° at θ(lab) =90°.

result is (0.12±0.01) for the ratio of the number of O^{16} atoms to C^{12} atoms in the target.

In Fig. 6 is shown a pulse-height spectrum of protons scattered at an angle of 90° to the incident beam. This spectrum illustrates the method used to obtain peak intensities in a case where the level spacing is comparable to the energy resolution. It is observed that the NaI(Tl) spectrometer response to an isolated proton peak for a thin target is well described by a Gaussian shape. The width of the Gaussian can be determined from the intense peaks which are known to correspond to isolated levels. With this knowledge it is fairly easy to separate partially resolved peaks and to subtract the background as long as the peaks are not too weak. The result of this procedure is illustrated by the Gaussian curves in Fig. 6 which indicate the intensities of the partially resolved peaks.

The deuteron group corresponding to the $B^{10}(p,d)B^{9}$ ground-state reaction was the only deuteron, triton, or alpha-particle group observed. The possible presence of other nonproton groups was checked for by repeating several angles with a 0.010-in. polystyrene absorber in front of the NaI(Tl) crystal.

The elastic peaks and the C^{12} 4.43- and 9.63-MeV levels provided a convenient energy calibration. With this calibration the energy of a peak could be located to about ±50 keV. The isotope to which a peak corresponds was determined by the shift in energy of the peaks with angle. For instance, the B^{10} peaks at 6.0 and 5.1 MeV shifted apart from the O^{16} 7.0- and 6.14-MeV peaks at forward and backward angles in quantitative agreement with the calculated shifts. With the exception of the B^{10} 5.1- and 6.0-MeV peaks, the B^{10} peaks indicated in Fig. 6 are believed to be due to single levels which have been observed previously.[25] There was no evidence for excitation of the B^{10} levels reported at 5.37, 5.58, and 6.42 MeV. The evidence for these states is from the $Be^{9}(d,n)B^{10}$ reaction alone, and seems to be rather meager.[25] These states were not observed in a recent high resolution study of the $B^{11}(He^{3},\alpha)B^{10}$ reactions.[36]

The angular distributions for the B^{10} excited states were obtained in the same manner as the B^{10} ground state. The results are given in Table III. The angular distributions of the first three excited states and the 6.0-MeV group are shown in Fig. 7. The cross sections given in Table III and the cross section scale in Fig. 7 may contain an additional systematic error of 15%. Except for the 5.1- and 6.0-MeV groups which will be discussed below, the excitation energies are from the literature.[25]

The 3.58-MeV peak was obscured at 28° and 30° by the $H(p,p)H$ peak, and at backward angles by the C^{12} 4.43-MeV level group. The 4.77-MeV peak was obscured at 20° by $H(p,p)H$ and at 110° to 125° by oxygen contamination. The intensities of the O^{16} groups at

[36] A. Gallman, D. E. Alburger, and D. H. Wilkinson (to be published).

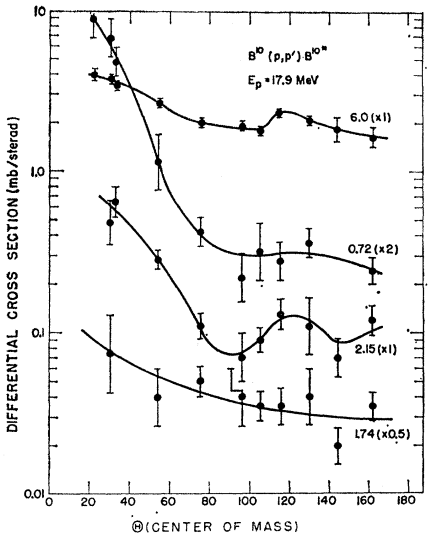

FIG. 7. Angular distributions of the first three levels of B^{10} and the 6.0-MeV proton group. The cross-section scale has an uncertainty of 15% in addition to the errors assigned to the individual points.

6.14 and 7.0 MeV were estimated from the $O^{16}(p,p')O^{16}$ angular distributions of Hornyak and Sherr[5] which were taken at 19 MeV, from runs taken at several angles with a Mylar ($C_{10}O_4H_8$) target at 17.9 MeV, and from the intensities of these O^{16} groups at those angles at which they were resolved from the B^{10} and C^{12} groups. These estimates were used to obtain the intensity of the B^{10} 5.1-MeV group which was unresolved from the O^{16} 6.14-MeV group between 70° and 110°. The B^{10} 5.1-MeV group and the O^{16} 6.14-MeV group were of about equal intensity at these angles. The B^{10} 6.0-MeV group had 8% O^{16} contamination at 20°, 5% at 28° and 30°, and a few percent or less at larger angles. The large errors associated with most of the cross sections given in Table III illustrate the need for better energy resolution in order to study a spectrum as complicated as that of B^{10}.

Discussion

The level scheme[25] of B^{10} is shown in Fig. 8. The 5.37-MeV level is not shown and the 5.58- and 6.42-MeV levels are indicated as being uncertain because of the recent $B^{11}(He^3,\alpha)B^{10}$ work.[36] A level has recently been found[37] at 5.18-MeV in B^{10}. The 5.18-MeV level, which is not shown in Fig. 8, has a width of ~200 keV and is assigned $J^\pi=1^{(+)}$, $T=0$. This level probably belongs to a doubly excited shell-model configuration[38] and therefore should be excited very weakly by the (p,p') reaction. It was not observed in a recent high-resolution study of the $B^{10}(p,p')B^{10}$ reaction made with 10-MeV protons.[39]

The proton group corresponding to an excitation of 5.14±0.06 MeV could have appreciable contributions from both the 5.11- and 5.16-MeV levels. The group corresponding to an excitation of 6.04±0.05 MeV is too narrow to have appreciable contributions from the B^{10} 5.93- and 6.16-MeV levels so that at least one-half of the cross section of 29.6±2 mb measured for this group is due to the 6.04-MeV level.

The present results can be compared to $B^{10}(\alpha,\alpha')B^{10}$ data[40] obtained at α-particle energies at 37.5 and 43 MeV. In this work the 2.15-, 3.59-, 4.77-, and 6.0-MeV levels were observed. The resolution was not sufficient to separate the 0.72-MeV level from the ground-state group or to tell which of the levels near 6.0 MeV in B^{10} were contributing to the reaction cross section. The 2.15-, 3.59-, and 4.77-MeV levels were excited with approximately (within a factor of 2) equal cross section while the 6.0-MeV group was ~5 to 10 times as intense. Thus, where a comparison is possible, the (α,α') results are in good agreement with the (p,p') results. The 5.1-MeV group seen in (p,p') was not observed in (α,α'). This gives some indication that this group is due, at least partially, to the $T=1$ 5.16-MeV level.

All the B^{10} cross sections are considerably smaller than the $Be^9(p,p')Be^9$ (2.43-MeV level) cross section. This is presumably mainly due to the large spin of the B^{10} ground state. For the direct interaction mechanism, the (p,p') cross section is proportional to $(2J_1+1)/(2J_0+1)$, where J_1 is the spin of the excited state and J_0 is the spin of the ground state. Thus, for example, the $Be^9(p,p')Be^9$ (2.43-MeV level) cross section is

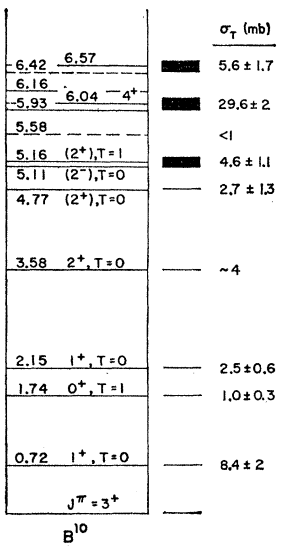

FIG. 8. Energy levels of B^{10}. The spin-parity assignments are from references 25, 36, and 37. The levels observed below 5-MeV excitation are indicated. The uncertainty in excitation energy of the three lowest energy proton groups and the total (p,p') cross sections for the proton groups are also indicated.

[37] E. L. Sprenkel, J. W. Olness, and R. E. Segel, Phys. Rev. Letters **7**, 174 (1961).
[38] W. W. True and E. K. Warburton, Nuclear Phys. **22**, 426 (1961).
[39] B. H. Armitage and R. E. Meads, Nuclear Phys. **33**, 494 (1962).
[40] P. C. Robison, thesis, University of Washington, 1958 (unpublished); G. W. Farwell and P. C. Robison (to be published).

TABLE IV. Experimental results for $Ne^{20}(p,p')Ne^{20*}$ in the laboratory and center-of-mass systems. The angles are in degrees and the differential cross sections in mb/sr.

		Excitation energy (MeV)											
		1.63			4.25			4.97			5.63±0.07		
θ(lab)	θ(c.m.)[a]	$\sigma(\theta)_{lab}$	Δ(%)	$\sigma(\theta)_{c.m.}$	$\sigma(\theta)_{lab}$	Δ(%)	$\sigma(\theta)_{c.m.}$	$\sigma(\theta)_{lab}$	Δ(%)	$\sigma(\theta)_{c.m.}$	$\sigma(\theta)_{lab}$	Δ(%)	$\sigma(\theta)_{c.m.}$
15	15.8	18.0	9	16.3	4.3	20	3.9	1.3	46	1.2	6.3	19	5.6
20	21.1	18.6	6	16.9	5.2	19	4.7	1.2	33	1.1	7.9	9	7.1
30	31.6	18.2	5	16.6	7.2	10	6.5	3.2	16	2.0	7.7	7	6.9
40	42.1	17.0	6	15.7	3.8	12	3.5	2.0	28	1.8	5.4	7	4.9
55	57.5	11.7	13	11.0	...	...	...	...	...	...	...	...	...
60	62.9	6.7	8	6.4	3.4	10	3.2	2.6	14	2.4	4.3	9	4.0
65	67.8	4.9	8	4.7	...	...	...	...	...	...	...	...	...
75	78.2	5.2	8	5.1	3.4	13	3.3	1.6	19	1.5	2.2	11	2.1
90	93.3	5.8	7	5.8	1.7	18	1.7	1.0	40	1.0	2.1	17	2.1
105	108.2	5.5	7	5.7	1.0	30	1.0	0.3	67	0.3	1.8	20	1.8
120	122.9	4.4	9	4.7	1.2	29	1.3	0.4	57	0.4	1.6	29	1.7
140	142.1	3.6	11	3.9	0.8	25	0.9	0.4	50	0.4	1.9	21	2.1
150	151.6	3.3	11	3.6	1.0	20	1.1	0.5	45	0.5	2.1	17	2.3
160	161.1	3.1	10	3.4	0.8	25	0.9	0.5	40	0.6	1.8	20	2.0
		Excitation energy (MeV)											
		7.45±0.08			7.85±0.08			9.20±0.09			10.0±0.10		
θ(lab)	θ(c.m.)[a]	$\sigma(\theta)_{lab}$	Δ(%)[b]	$\sigma(\theta)_{c.m.}$	$\sigma(\theta)_{lab}$	Δ(%)[b]	$\sigma(\theta)_{c.m.}$	$\sigma(\theta)_{lab}$	Δ(%)[b]	$\sigma(\theta)_{c.m.}$	$\sigma(\theta)_{lab}$	Δ(%)[b]	$\sigma(\theta)_{c.m.}$
20	21.4	5.0	10	4.4	4.4	12	3.8	4.9	12	4.3	...	...	...
40	42.6	3.2	15	2.9	1.5	20	1.3	1.8	20	1.6	5.0	13	4.5
60	63.6	2.3	20	2.1	1.0	20	0.9	...	...	...	...	...	...
90	94.2	1.6	20	1.6	0.6	30	0.6	1.2	25	1.2	2.2	20	2.2
120	123.6	0.8	25	0.9	0.6	30	0.6	0.4	40	0.4	...	...	...
140	142.7	0.6	30	0.7	0.4	40	0.5	...	...	...	...	...	...
160	161.4	1.0	25	1.2	1.1	20	1.3	0.5	30	0.6	1.2	25	1.4

[a] Mean value for the four levels, ±0.3° at θ(lab) = 90°.
[b] Rough estimates, mostly due to graphical analysis.

intrinsically stronger by a factor of 3.5 than the $B^{10}(p,p')B^{10}$ (0.72-MeV level) cross section.

The lifetime of the B^{10} 0.72-MeV level has been measured,[41] it corresponds to an $E2$ transition strength of $|M(E2)|^2=3.17\pm0.07$ in Weisskopf units with $r_0=1.2$ F.[42] Assuming that the (p,p') cross section is proportional to $[(2J_1+1)/(2J_0+1)]\times|M(EL)|^2$, the transition strength $|M(E2)|^2$ of ground-state transitions from the other positive parity levels for which $L=2$ is expected will be given by

$$|M(E2)|^2=\frac{3}{(2J_1+1)}\frac{\sigma_T(p,p')}{8.4\pm2}(3.17\pm0.07), \quad (2)$$

where J_1 is the spin of the level and $\sigma_T(p,p')$ is the cross section for the level in mb. This relation predicts $|M(E2)|^2=1\pm0.35$ in Weisskopf units for the 2.15-MeV level. This result will be discussed in the next section. The 5.16- and 6.04-MeV levels are the only ones besides the 0.72-MeV level for which some information on the $E2$ ground-state transition is available. For these levels $Li^6(\alpha,\gamma)B^{10}$ results[43] indicate $\Gamma(E2)\approx2\times10^{-3}$ eV and $\Gamma(E2)/\Gamma(M1)=9$, respectively. The former corresponds to $|M(E2)|^2\approx0.5$ while the latter implies that $|M(E2)|^2$ is relatively large. Equation (2) indicates $|M(E2)|\approx1$ for the 5.16-MeV level and $|M(E2)|^2\approx3.7$ for the 6.04-MeV level if the cross sections observed are entirely due to those levels. Thus, the relative (p,p') cross sections for the states of B^{10} with known $E2$ ground-state strengths are consistent with Eq. (2).

In the usual form of the direct-interaction (p,p') reaction, the 0^+ B^{10} 1.74-MeV level can only be excited via spin-flip terms since a $3^+\rightarrow0^+$ transition cannot proceed by an EL interaction otherwise. Thus the cross section of 1 mb for excitation of the B^{10} 1.74-MeV level gives some measure of the contribution of the spin-dependent part of the interaction to the (p,p') cross section, and from its relative magnitude it would seem that only the strongest $E2$ rates in B^{10} are enhanced enough to make Eq. (2) meaningful. For the weaker transitions Eq. (2) could be greatly in error since the spin-dependent and spin-independent contributions can add destructively as well as constructively.

C. Ne^{20}

Experimental Results

The Ne^{20} target consisted of natural neon gas (90.8% Ne^{20}) at 10 mm Hg pressure. The gas was contained in a 4-in.-diam cylinder with brass ends. The cylinder wall consisted of a 0.0005-in. Mylar window glued

[41] J. Lowe, C. L. McClelland, and J. V. Kane, Phys. Rev. **126**, 1811 (1962).
[42] D. H. Wilkinson in *Nuclear Spectroscopy*, edited by F. Ajzenberg-Selove (Academic Press Inc., New York, 1960), Part B, pp. 852–889.
[43] L. Meyer-Schützmeister and S. S. Hanna, Phys. Rev. **108**, 1506 (1957).

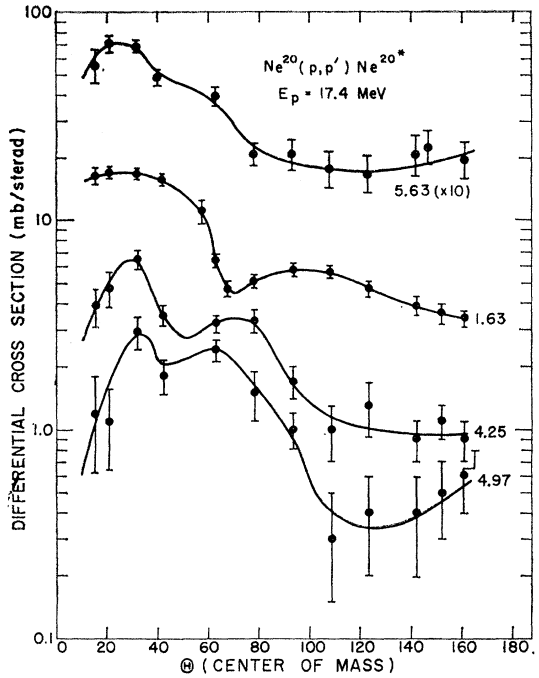

FIG. 9. Angular distributions of the first four levels of Ne^{20}. The cross-section scale has an uncertainty of 10% in addition to the errors assigned to the individual points.

with epoxy resin around the entire circumference. The brass ends were held rigidly apart with three brass rods placed at 120° intervals around the circumference of the cylinder. The scattering volume was defined by a standard slit system of 3.5° angular aperture placed in front of the NaI(Tl) crystal. Enough absorber was placed in front of the NaI(Tl) crystal to degrade deuterons, etc., out of the energy region of interest. The energy resolution with this arrangement was 2.3% for 17-MeV protons. The cyclotron beam energy was adjusted so that the energy of the proton beam at the center of the gas cell was 17.4 MeV corresponding to a center-of-mass energy of 16.6 MeV. This demanded a cyclotron energy of about 17.5 MeV. The differential cross sections were obtained from the known geometry, the Ne^{20} gas pressure, and the total integrated proton charge.

The experimental results are given in Table IV. The angular distributions of the first four excited states are shown in Fig. 9. The cross sections given in Table IV and the cross-section scale in Fig. 9 both contain an additional uncertainty which is estimated to be 10%.

The excitation energies of the first three levels in Table III are from the literature,[25] while the excitation energies of the remaining groups are measured and have uncertainties between 70 and 100 keV. None of the first six proton groups observed had widths larger than that expected so that it is probable that the first six groups are due to single isolated levels.

Discussion

The level scheme of Ne^{20} is shown in Fig. 10. It is taken from Ajzenberg-Selove and Lauritsen[25] and from recent work of Litherland *et al.*,[44] who showed that the collective model gives a good account of the low-lying levels of Ne^{20}.

As is expected on a rotational model in an even-even nucleus, the first excited state has $J^\pi=2^+$ and has the largest (p,p') cross section. The lifetime of this state has been measured to be $(5.6_{-1.2}^{+2.8})\times10^{-13}$ sec[45] and $(7.6\pm3.3)\times10^{-13}$ sec.[25] Averaging these values gives $|M(E2)|^2=33_{-12}^{+6}$. The average value of $|M(E2)|^2$ for light nuclei is ~5 so that the Ne^{20} 1.63 $\rightarrow$ 0 transition is greatly enhanced. It would appear that the 4.25 $\rightarrow$ 0 $E4$ transition is also enhanced since the cross section for the $Ne^{20}(p,p')Ne^{20}$ (4.25-MeV level) reaction seems quite large for $L=4$.

Inelastic scattering from Ne^{20} has been studied previously using 18-MeV α-particles.[46] Alpha groups identified as corresponding to levels of Ne^{20} at 1.63, 4.25, 4.97, 5.81 (or 5.63), and 7.2 MeV were observed

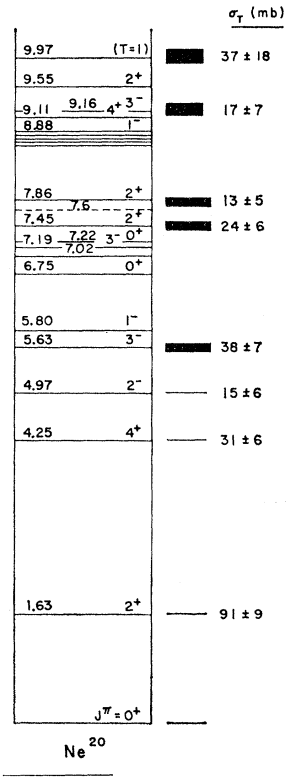

FIG. 10. Energy levels of Ne^{20}. The spin-parity assignments are from references 25 and 44. The uncertainty in excitation energy is indicated for all but the three highest energy proton groups. The total (p,p') cross sections for the proton groups are also shown.

[44] A. E. Litherland, J. A. Kuehner, H. E. Gove, M. A. Clark, and E. Almqvist, Phys. Rev. Letters **7**, 98 (1961); and *Proceedings of the Rutherford Jubilee International Conference, Manchester, 1961* (Academic Press Inc., New York, 1961).

[45] M. A. Clark, H. E. Gove, and A. E. Litherland, *Proceedings of the Rutherford Jubilee International Conference, Manchester, 1961* (Academic Press Inc., New York, 1961); Can. J. Phys. **39**, 1241 (1961).

[46] L. Seidlitz, E. Bleuler, and D. J. Tendam, Phys. Rev. **110**, 682 (1958).

TABLE V. Experimental results for the elastic scattering of 17.3-MeV protons by Mg^{25}. The angles are in degrees and the cross sections are in mb/sr.

θ(lab)	$\sigma(\theta)_{lab}$	θ(c.m.)	$\sigma(\theta)_{c.m.}$	$\Delta(\%)$
15	1890	15.6	1750	12
25	510	26.0	475	10
40	17.5	41.5	16.5	12
55	35.6	56.9	34.0	10
70	40.5	72.2	39.5	10
90	8.7	92.3	8.7	8
110	7.0	112.2	7.2	8
130	6.8	131.8	7.2	9
150	5.9	151.2	6.3	8
165	3.2	165.6	3.5	10

using nuclear emulsions. If, in reality, the groups identified with the 5.81- (or 5.63-), and 7.02-MeV levels correspond to the fifth and sixth groups seen in the present work then the (α,α') results are in remarkable accord with the present (p,p') results—the integrated (α,α') cross sections being in almost 1:1 correspondence with the total cross sections given in Fig. 10.

If it were not for the (α,α') results, the excitation of the 2^- 4.97-MeV level in (p,p') would be ascribed to the spin-dependent interaction which could cause $L=1$ and 3 transitions. However, this level is seen with about the same cross section (relative and absolute) in the (α,α') reaction and, since the α particle has zero spin, it is difficult to envisage a one-step direct interaction mechanism responsible for its excitation. Whatever the reaction mechanism responsible for the formation of the 4.97-MeV level, its excitation in the (p,p') and (α,α') reactions warn us, as does the $B^{10}(p,p')B^{10}$ (1.74-MeV level) reaction, that only for the strongest (p,p') transitions can we hope to find proportionality with the EL transition rates for the proton energy range of 17 to 20 MeV.

The (p,p') transition to the 3^- 5.63-MeV level is the second strongest one observed in Ne^{20}, indicating collective enhancement of the $5.63 \rightarrow 0$ $E3$ transition. Litherland *et al.*[44] give two alternative explanations of this level. It might belong to a negative parity band explained as rotations of the Ne^{20} nucleus which is undergoing surface octupole vibrations, or to a negative parity band based upon states of particle excitation. Since the former explanation would be expected to lead to larger enhancement of the $E3$ ground-state transition, the present results give some support to that alternative.

The next two (p,p') transitions in Fig. 10 are presumably mainly to 2^+ states. Their cross sections are much smaller than to the first excited state and about the same as to the 2^- 4.97-MeV level. Thus, there is no evidence from (p,p') for collective enhancement of these $E2$ transitions in accord with the rotational model since these levels are not members of the ground state band. The lowest energy proton group observed in $Ne^{20}(p,p')Ne^{20}$ corresponds to an excitation energy of 10.0 ± 0.1 MeV. The only known state of Ne^{20} near this energy is at 9.97 ± 0.1 MeV and this level has been tentatively assigned $T=1$.[25] If so, it is most likely the analog of the F^{20} ground state which has $J^\pi=2^+$.[47] Since a $\Delta T=1$, $E2$ transition in a self-conjugate nucleus cannot have collective enhancement, the rather large cross section which is observed seems surprising. However, the uncertainty in this cross section is quite large and the cross section could, in fact, be no larger than that of the 2^-, 4.97-MeV level.

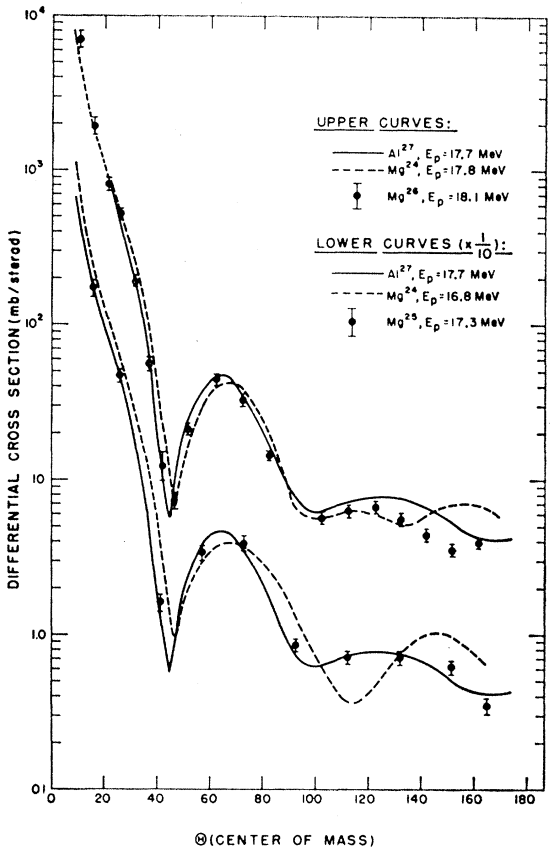

FIG. 11. Elastic scattering angular distributions for Mg^{24}, Mg^{25}, Mg^{26}, and Al^{27}. The Mg^{24} data are from reference 7, the Mg^{25} and Mg^{26} data are from the present work, and the Al^{27} data are from reference 22. As described in the text, the $Mg^{25}(p,p')Mg^{25*}$ cross sections were obtained by normalizing the Mg^{25} angular distribution to the others shown in the figure. For the Mg^{25} data only, the cross section scale has an uncertainty of 15% due to this normalization.

D. Mg^{25}

Experimental Results

The Mg^{25} target was prepared by vacuum evaporation of Mg enriched in Mg^{25} onto a 0.0005-in. polystyrene foil. The composition of the Mg foil was 5.5% Mg^{24}, 93.5% Mg^{25}, and 1.0% Mg^{26}. A bombarding energy of 17.3 MeV was used in this work, corresponding to 16.7 MeV in the center-of-mass system. The

[47] E. Freiberg and V. Soergel, Z. Physik **162**, 114 (1961).

TABLE VI. Experimental results for $Mg^{25}(p,p')Mg^{25*}$ in the laboratory and center-of-mass systems. The angles are in degrees and the differential cross sections in mb/sr.

		Excitation energy (MeV)									
		1.61			2.7		3.4		4.0		
θ(lab)	θ(c.m.)[a]	$\sigma(\theta)_{lab}$	Δ(%)	$\sigma(\theta)_{c.m.}$	$\sigma(\theta)_{lab}$	$\sigma(\theta)_{c.m.}$	$\sigma(\theta)_{lab}$	$\sigma(\theta)_{c.m.}$	$\sigma(\theta)_{lab}$	$\sigma(\theta)_{c.m.}$	Δ(%)[b]
15	15.6	12.7	4.7	11.7	3.2	3.0	3.5	3.2	3.1	2.9	15
25	26.1	7.3	4.8	6.8	1.7	1.6	...	...	1.9	1.8	15
40	41.6	5.9	5.1	5.5	1.6	1.5	2.1	2.0	1.7	1.6	15
55	57.1	4.6	5.5	4.4	1.1	1.1	1.5	1.4	1.5	1.4	15
70	72.4	3.8	5.3	3.7	1.0	1.0	1.4	1.4	1.6	1.6	15
90	92.5	3.5	4.9	3.5	0.8	0.8	1.5	1.5	1.4	1.4	12
110	112.4	2.2	9.0	2.2	0.4	0.4	1.2	1.2	0.9	0.9	15
130	131.9	1.3	11.0	1.4	0.4	0.4	1.0	1.1	0.8	0.9	15
150	151.3	0.5	10.0	0.6	0.6	0.7	0.8	0.9	1.2	1.3	15
165	165.6	...	...	...	0.8	0.9	0.4	0.5	1.2	1.3	20

[a] Average value for the four levels ($\pm$0.1°).
[b] Rough estimates for the 2.7-, 3.4-, and 4.0-MeV levels, mostly due to graphical analysis.

absolute cross sections for $Mg^{25}(p,p')Mg^{25}$ were determined by normalizing the $Mg^{25}(p,p)Mg^{25}$ angular distribution, obtained from the integrated charge, to angular distributions for the Mg^{24}, Mg^{26}, and Al^{27} ground states. This procedure was adopted because the target was inadvertently destroyed before it could be weighed. As can be seen in Fig. 11, the maximum at about 70° in the (p,p) angular distributions for masses 24 to 27 and $E_p=17$ to 18 MeV are between 40 and 50 mb/sr. Because of the similarity of the curves in Fig. 11 near 70°, it was considered safe to assume the $Mg^{25}(p,p)Mg^{25}$ angular distribution had the same behavior. The normalization used is shown by the experimental points in the lower set of curves in Fig. 11. The $Mg^{25}(p,p)Mg^{25}$ results are given in Table V. The cross-section scale of Fig. 11 for the $Mg^{25}(p,p)Mg^{25}$ angular distribution and the results of Table V have an estimated additional uncertainty of 15% due to this normalization procedure.

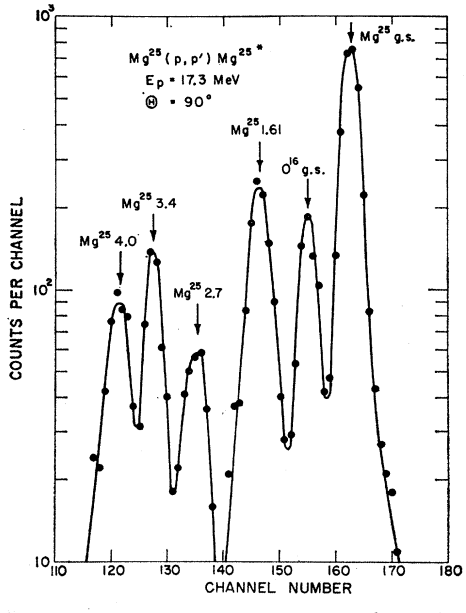

FIG. 12. Pulse height spectrum of $Mg^{25}+p$ observed at 90° to the proton beam at a proton energy of 17.3 MeV. The peaks are labeled by the isotope and excitation energy to which they are assumed to belong.

A pulse-height spectrum taken at 90° to the beam is shown in Fig. 12. The reaction was not investigated above an excitation energy of 4.5 MeV.

The target contained some oxygen contamination. The ratio of O^{16} atoms to Mg^{25} atoms was determined to be 0.077 by comparing the intensities of the elastic peaks at backward angles. In the same manner the number of C^{12} atoms was determined to be a few percent of the number of Mg^{25} atoms. At backward angles, it was necessary to correct the peak intensities of the Mg^{25} 1.61- and 2.7-MeV groups for the presence of the C^{12} and O^{16} elastic peaks. This was done using the $O^{16}(p,p)O^{16}$ angular distribution taken at a proton energy of 17.6 MeV by Maxson[33] (see Fig. 3) and Peelle's data[3] for the $C^{12}(p,p)C^{12}$ angular distribution at a proton energy of 17.4 MeV. The target was maintained in a vacuum at all times to keep the O^{16} contamination constant.

The experimental results for the four Mg^{25} proton groups shown in Fig. 12 are given in Table VI and the angular distributions are shown in Fig. 13. The cross-section scale in Fig. 13 and the cross sections in Table VI all have an uncertainty of 15%. The excitation energy of the 1.61-MeV group is from the literature,[48] while the other three excitation energies are measured values ($\pm$100 keV). The 1.61-MeV group corresponds to a single Mg^{25} level, the other three groups contain possible contributions from more than one level. This will be discussed further below.

Discussion

The level scheme of Mg^{25} is shown in Fig. 14 which is taken from Endt and Braams,[48] from Hinds, Marchant, and Middleton,[49] and from Litherland *et al.*[50]

[48] P. M. Endt and C. M. Braams, Revs. Modern Phys. **29**, 683 (1957).
[49] S. Hinds, H. Marchant, and R. R. Middleton, Proc. Phys. Soc. (London) **78**, 473 (1961).
[50] A. E. Litherland, H. McManus, E. B. Paul, D. A. Bromley,

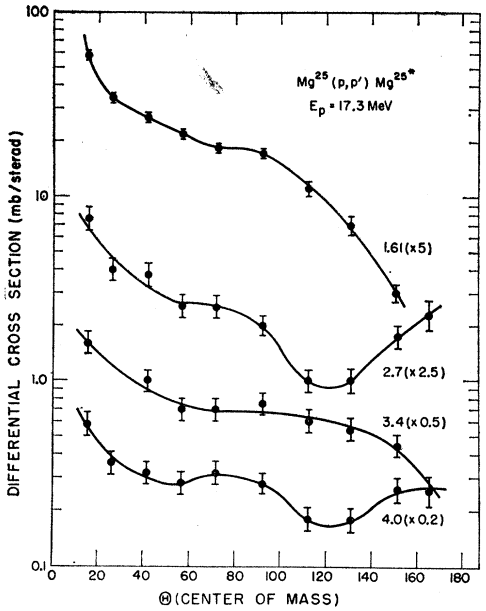

FIG. 13. Angular distributions of the four Mg^{25} proton groups observed. The cross section scale has an uncertainty of 15% in addition to the errors assigned to the individual points.

Of the light nuclei, the collective model has had the most noticeable success[50] in Mg^{25}–Al^{25} and we shall see that this model gives an excellent qualitative explanation of the relative (p,p') cross sections.

The rotational, $K=5/2$, band built on the ground state has its first excited state at 1.61 MeV. For this band the odd (13th proton) is in Nilsson orbit[51] No. 5, all lower orbits being filled. The states at 0.58, 0.98, and 1.96 MeV in Mg^{25} are identified as members of the $K=1/2$ band with the odd neutron in orbit No. 9. It is expected that there is little mixing between this $K=1/2$ band and the $K=5/2$ ground-state band.[50,52] Thus, Coulomb excitation and the (p,p') reaction should show little or no collective enhancement of the $K=1/2$ band, but both should show a strong enhancement of the 1.61-MeV state. This prediction is in excellent accord with the relative (p,p') total cross sections shown in Fig. 14 for the first four levels of Mg^{25}. It is also in good accord with recent Coulomb excitation experiments[53] from which $E2$ transition strengths, $|M(E2)|^2$, in Weisskopf units of 0.4, 1.2, and 19 are extracted for the Mg^{25} 0.58-, 0.98-, and 1.61-MeV levels, respectively. The quoted[53] uncertainties in these transition strengths are about 25%. Assuming proportionality between $\sigma_T(p,p')$ and $|M(E2)|^2$ the $|M(E2)|^2$ given above and the $\sigma_T(p,p')$ given in Fig. 14 for the Mg^{25} 1.61-MeV level lead to predicted values of $\sigma_T(p,p')$ of 0.2 and 1.3 mb for the Mg^{25} 0.58- and 0.98-MeV levels. These values are consistent with the upper limits given in Fig. 14 for these levels.

The inelastic scattering of 15-MeV deuterons from Mg^{25} has been studied by Blair and Hamburger.[54] Their results for these levels are in good agreement with ours; they found that the excitation of the levels at 0.58, 0.98, and 1.96 MeV was less than 1/10 of the Mg^{25} 1.61-MeV level excitation. They also found that a level at 3.40 MeV was the only other level which was excited strongly and for this reason conjectured that this level was the $9/2^+$ member of the $K=5/2$ ground-state band instead of being $3/2^-$ as other evidence indicated.[50] Since their work was completed, the 3.40-MeV level was found to be a doublet with some indication that the second member was $9/2^+$.[49] The collective model predicts 0.35 for the ratio of the cross sections for the formation of the $9/2^+$ and $7/2^+$ states of the $K=5/2$ band. Assuming the 3.40-MeV level they excited was the $9/2^+$ state, they found 0.41 for this ratio at $\theta_{lab}=29.7°$. The present results give 0.41 for the (p,p') total cross-section ratio if the Mg^{25} $3/2^-$ state has negligible cross section. Thus, agreement

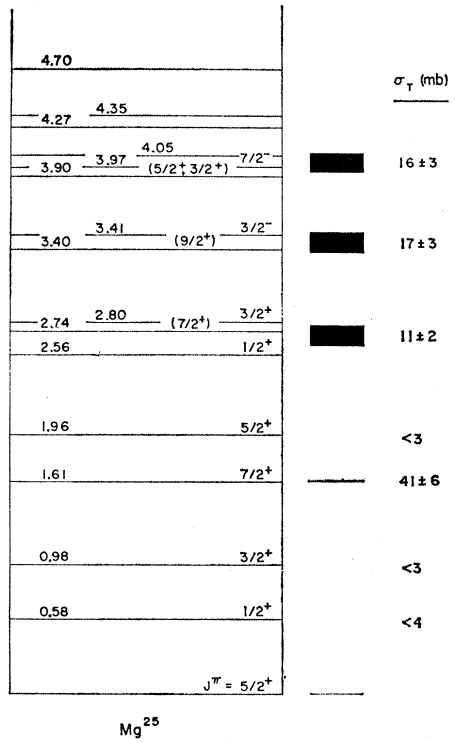

FIG. 14. Energy levels and total (p,p') cross sections of Mg^{25}. The information on the energy levels is taken from references 48, 49, and 50.

and H. E. Gove, Can. J. Phys. **36**, 378 (1958); A. E. Litherland, H. E. Gove, and A. J. Ferguson, Phys. Rev. **114**, 1312 (1959).

[51] S. G. Nilsson, Kgl. Danske Videnskab. Selskab, Mat.-fys. Medd. **29**, No. 16 (1955).

[52] D. A. Bromley (private communication).

[53] D. S. Andreev, V. A. Vasillev, G. M. Gusinskii, K. I. Brokhina, and I. Kh. Lembert, Izvest. Akad. Nauk. S. S. S. R., Ser. Fiz. **25**, 832 (1961).

[54] A. G. Blair and E. W. Hamburger, Phys. Rev. **122**, 566 (1961).

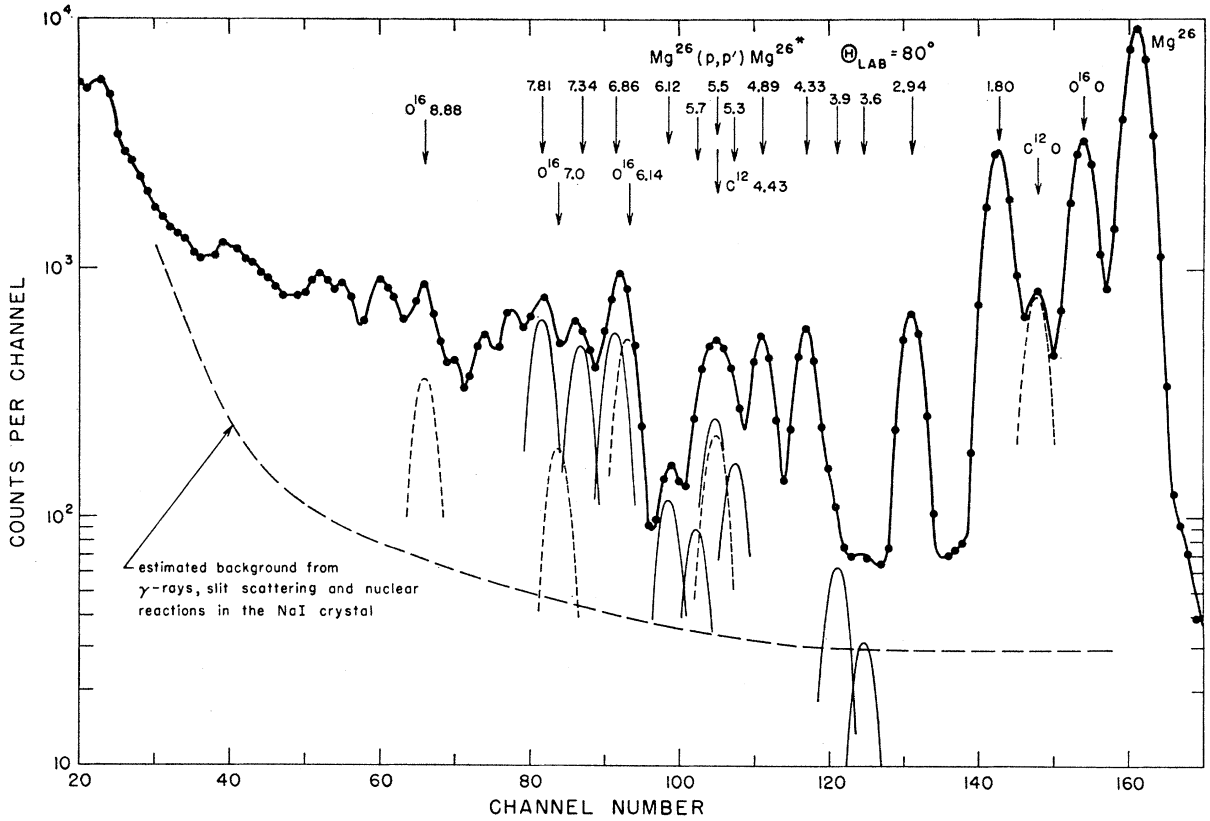

FIG. 15. Pulse-height spectrum of $Mg^{26}+p$ observed at 80° to the proton beam at a proton energy of 18.1 MeV. The peaks are labeled by the isotope and excitation energy to which they are assumed to belong. The Gaussian curves indicate the assumed shapes and intensities of unresolved peaks.

with the rotational model for both (p,p') and (d,d') is quite good.

In the present work the triplets near 2.7 and 4.0 MeV were not resolved and so the total cross sections given for these groups are, in both cases, for the sum of these levels. The levels at 2.56, 2.80, and possible 3.90 MeV are identified with the $K=1/2$ band of orbit No. 11.[50] The mixing of this band with the $K=5/2$ ground-state band is expected to be considerably more than for the band of orbit No. 9.[50,52] If so, these levels should be excited more strongly in inelastic scattering than the first, second, fourth, and 2.74-MeV (orbit No. 9) level. The (d,d') results,[54] in which these triplets were resolved, show this to be the case. The relative cross sections for the sums of the three levels in each triplet obtained in the (d,d') work are in fair agreement with the relative cross sections for the 2.7- and 4.0-MeV groups obtained in the present work.

TABLE VII. Experimental results for the elastic scattering of 18.1-MeV protons by Mg^{26}. The angles are in degrees and the cross sections are in mb/sr.

θ(lab)	$\sigma(\theta)_{lab}$	θ(c.m.)	$\sigma(\theta)_{c.m.}$	Δ(%)
10	7600	10.38	7053	15
15	2120	15.56	1973	5
21	870	21.78	811	4
25	560	25.92	523	6
30	205	31.09	192	6
35	60.1	36.25	56.5	5
40	13.0	41.40	12.3	20
45	7.8	46.54	7.4	10
50	22.5	51.67	21.4	7
60	48.0	61.89	46.3	3
70	33.6	72.04	32.8	3
80	14.4	82.15	14.2	3
90	6.37	92.18	6.37	3
100	5.70	102.15	5.78	4
110	6.08	112.04	6.24	3
120	6.43	121.89	6.68	3
130	5.25	131.67	5.52	3
140	4.10	141.40	4.35	3
150	3.33	151.09	3.56	3
160	3.59	160.75	3.86	3

E. Mg^{26}

Experimental Results

Mg^{26} was bombarded with a proton beam with an energy at the center of the target of 18.1±0.1 MeV, corresponding to 17.4 MeV in the center-of-mass system. The Mg^{26} target was produced like the Mg^{25} target. The admixture of other magnesium isotopes was less than 2%. The target weighed 4.5±2 mg/cm², where the quoted error reflects the nonuniformity of

TABLE VIII. Experimental results for $Mg^{26}(p,p')Mg^{26*}$ in the laboratory and center-of-mass systems. The angles are in degrees and the differential cross sections in mb/sr.

		Excitation energy (MeV)					
		1.80			2.94		
θ(lab)	θ(c.m.)[a]	$\sigma(\theta)_{lab}$	Δ(%)	$\sigma(\theta)_{c.m.}$	$\sigma(\theta)_{lab}$	Δ(%)	$\sigma(\theta)_{c.m.}$
10	10.4	14.8	50	13.7	5.0	50	4.61
15	15.6	18.0	6	16.7	4.3	20	3.97
21	21.9	15.2	3	14.1	3.45	7	3.20
25	26.0	13.6	6	12.6	...	...	...
30	31.2	11.9	6	11.1	2.95	10	2.75
35	36.4	10.9	3	10.2	2.53	3	2.37
40	41.6	9.35	5	8.79	2.20	6	2.07
45	46.7	8.55	3	8.08	1.95	3	1.84
50	51.9	7.30	6	6.93	1.70	6	1.61
60	62.1	5.24	3	5.04	1.26	3	1.21
70	72.3	4.75	3	4.62	1.09	3	1.06
80	82.4	4.82	3	4.76	0.96	3	0.95
90	92.4	4.24	4	4.24	0.80	3	0.80
100	102.4	2.73	4	2.77	0.52	3	0.53
110	112.3	1.72	4	1.77	0.30	4	0.31
120	122.1	2.24	3	2.34	0.26	4	0.27
130	131.9	2.71	3	2.84	0.32	4	0.34
140	141.6	2.70	3	2.88	0.44	4	0.47
150	151.2	2.06	10	2.21	0.56	6	0.60
160	160.8	1.35	15	1.46	0.70	8	0.76

		Excitation energy (MeV)								
		4.33			4.89			5.3+5.5+5.7		
θ(lab)	θ(c.m.)[b]	$\sigma(\theta)_{lab}$	Δ(%)	$\sigma(\theta)_{c.m.}$	$\sigma(\theta)_{lab}$	Δ(%)	$\sigma(\theta)_{c.m.}$	$\sigma(\theta)_{lab}$	Δ(%)	$\sigma(\theta)_{c.m.}$
15	15.7	1.36	25	1.25	3.58	20	3.29	2.00	30	1.83
21	22.0	1.06	15	0.98	2.68	10	2.47	1.52	20	1.40
25	26.1	...	...	...	2.35	20	2.17	1.60	30	1.47
30	31.4	...	...	...	...	...	...	1.50	30	1.39
35	36.6	1.13	10	1.05	1.80	10	1.67	...	...	...
40	41.7	1.14	20	1.07	...	...	...	1.0	20	0.93
45	46.9	1.11	3	1.04	1.57	10	1.48	1.30	10	1.22
50	52.1	1.10	10	1.04	...	...	...	1.10	20	1.04
60	62.3	0.96	4	0.92	0.96	15	0.92	1.00	15	0.95
70	72.5	0.85	4	0.83	0.80	4	0.78	0.92	10	0.89
80	82.7	0.82	3	0.81	0.76	3	0.75	0.80	10	0.79
90	92.7	0.82	3	0.82	0.75	3	0.75	0.83	10	0.83
100	102.7	0.85	3	0.86	0.65	4	0.66	0.72	10	0.73
110	112.5	0.79	3	0.81	0.60	4	0.62	0.54	10	0.56
120	122.3	0.76	3	0.80	0.58	5	0.61	0.52	10	0.55
130	132.0	0.74	3	0.78	0.51	5	0.54	0.40	10	0.43
140	141.7	0.66	3	0.71	0.47	5	0.50	0.45	10	0.48
150	151.3	0.60	4	0.65	0.40	5	0.43	0.61	10	0.66
160	160.9	0.51	5	0.55	0.30	10	0.33	0.61	15	0.67

		Excitation energy (MeV)								
		6.85			7.34			7.81		
θ(lab)	θ(c.m.)[c]	$\sigma(\theta)_{lab}$	Δ(%)[d]	$\sigma(\theta)_{c.m.}$	$\sigma(\theta)_{lab}$	Δ(%)[d]	$\sigma(\theta)_{c.m.}$	$\sigma(\theta)_{lab}$	Δ(%)[d]	$\sigma(\theta)_{c.m.}$
15	15.8	1.20	25	1.09	1.10	40	1.00	1.94	30	1.76
21	22.1	1.10	18	1.01	1.55	20	1.41	1.52	15	1.38
25	...	...	...	...	...	...	...	...	...	...
30	...	...	...	...	...	...	...	...	...	...
35	36.7	1.11	15	1.03	1.46	15	1.35	1.71	10	1.57
40	...	...	...	...	...	...	...	...	...	...
45	47.1	1.16	10	1.08	1.23	20	1.15	1.39	10	1.29
50	...	...	...	...	...	...	...	...	...	...
60	62.5	0.86	10	0.82	0.95	20	0.90	1.11	10	1.06
70	72.7	0.79	15	0.76	0.94	10	0.91	0.97	10	0.94
80	82.9	0.80	15	0.79	0.78	10	0.77	0.96	10	0.94
90	92.9	0.71	15	0.71	0.83	10	0.83	0.91	15	0.91
100	102.9	0.79	20	0.80	0.80	15	0.82	0.66	20	0.67
110	112.7	0.55	20	0.57	0.68	15	0.71	0.66	15	0.68
120	122.5	0.66	20	0.69	0.59	20	0.62	0.74	20	0.78
130	132.2	0.40	20	0.43	0.61	20	0.65	0.82	15	0.88
140	141.9	0.36	15	0.39	0.68	20	0.74	0.79	20	0.86
150	151.5	0.36	15	0.39	0.81	20	0.89	0.84	20	0.92
160	161.0	0.48	20	0.53	0.72	25	0.79	0.87	20	0.96

[a] Mean value for the two levels, $\pm 0.3°$ at θ(lab) $=90°$.
[b] Mean value for the five levels, $\pm 0.3°$ at θ(lab) $=90°$.
[c] Mean value for the three levels, $\pm 0.3°$ at θ(lab) $=90°$.
[d] Rough estimates, mostly due to graphical analysis.

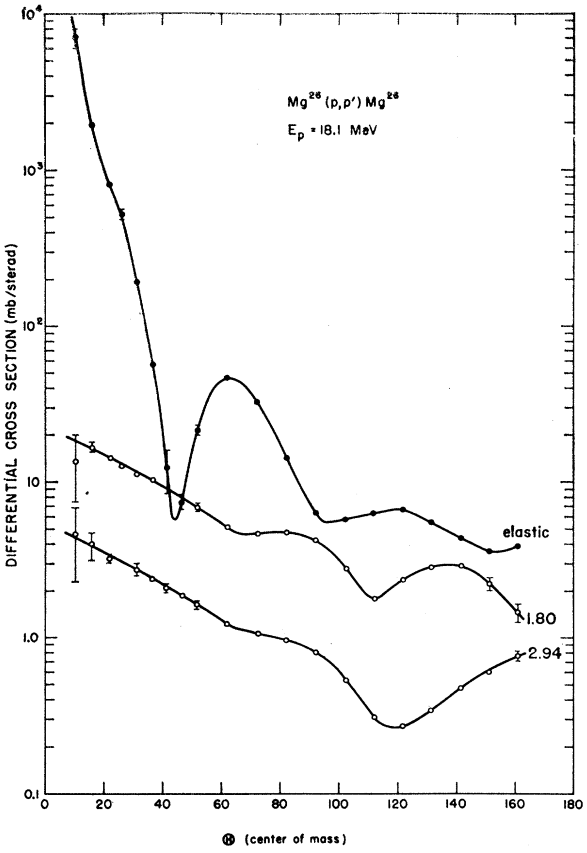

FIG. 16. Angular distributions of the elastic group and first two excited states of Mg^{26}. The cross section scale has an uncertainty of 10% in addition to the errors assigned to the individual points.

the target. The content of oxygen and carbon in the target was appreciable, as can be seen from Fig. 15. From the resolved O^{16} and C^{12} peaks an O^{16} contamination of 0.30 mg/cm^2 and a C^{12} contamination of 0.10 mg/cm^2 was computed, and corrected for in the determination of the differential cross sections.

The experimental results are given in Table VII and Table VIII. The excitation energies for the first four states were taken from the literature,[49] the excitation energies of the higher states were measured. The estimated error in the quoted values increases from ± 20 keV for the 4.33-MeV group to ± 70 keV for the 7.81-MeV group. The cross-section errors quoted in Tables VII and VIII are relative errors, and reflect uncertainties in the background subtraction and statistics. These errors are generally small for scattering from the low-lying states. However, uncertainties in the calibration of the charge integrator and the true target thickness may cause all cross sections to be systematically in error by $\pm 10\%$. Figure 16 is a

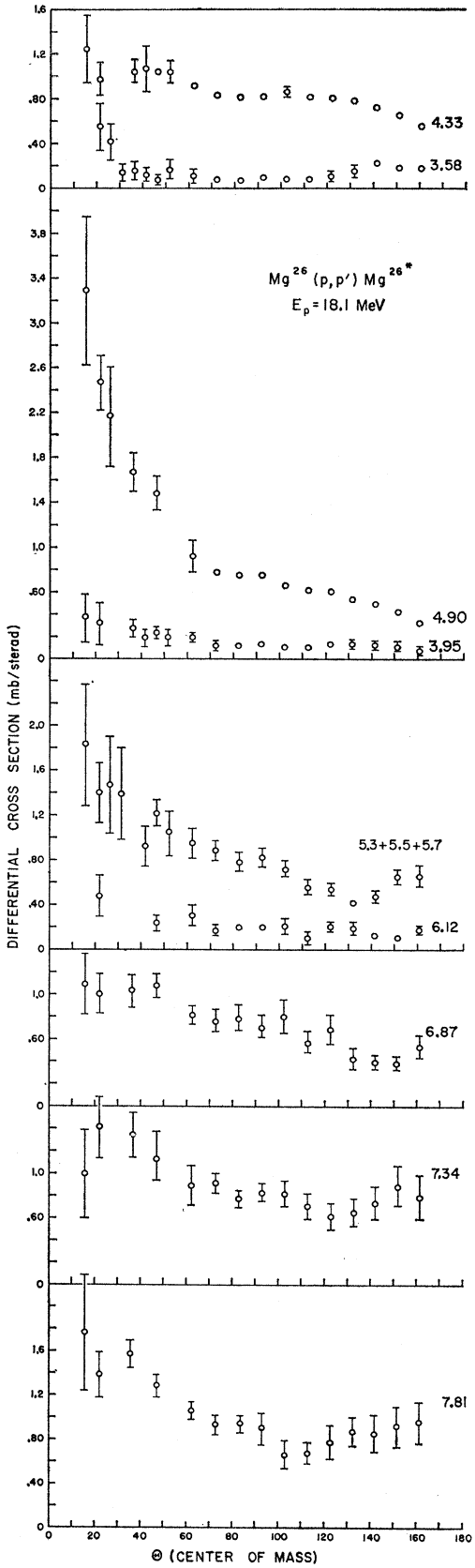

FIG. 17. Angular distributions for proton groups observed in $Mg^{26}+p$. The proton groups are labeled by the Mg^{26} excitation energies of the levels to which they correspond. The cross section scale has an uncertainty of 10% in addition to the errors assigned to the individual points.

logarithmic plot of the experimental differential cross sections for the ground state and the first two excited states. These angular distributions show much more structure than those for the higher excited states, which are shown in the linear plots of Fig. 17. Scattering from the states, at 3.58, 3.95, and 6.12 MeV is very weak, and the corresponding proton groups are frequently not resolved (see Fig. 15). Cross section estimates for these levels are given in Fig. 17 for the sake of completeness, but are not included in Table VIII.

The proton groups corresponding to the 5.3-, 5.5-, and 5.7-MeV states were rarely resolved from each other, but together they usually stand out as a broad peak; therefore, only the sum of their cross sections can be given. From the shape of the observed peaks it is estimated that the ratio of their total cross sections is about 3 to 4 to 2. All other cross sections reported here are derived from proton groups which were usually well resolved and not wider than about 340 keV, which was the energy resolution of this experiment. This suggests that these groups refer either to single states or to levels separated by less than about 100 keV.

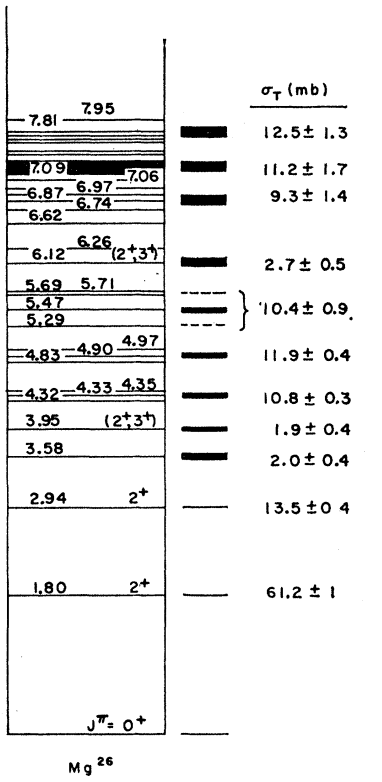

FIG. 18. Energy levels and total (p,p') cross sections of Mg^{26}. The information on the energy levels is taken from references 48 and 49. The uncertainties on the cross sections are relative, the absolute errors are all about 10%.

Discussion

The level scheme of Mg^{26} is shown in Fig. 18.[48,49] Blair and Hamburger[54] also studied the inelastic scattering of 15-MeV deuterons from Mg^{26}. Their relative cross section results, which are for excitation energies less than 5.5 MeV, are in qualitative agreement with our (p,p') results.

The rotational model has not been successful in interpreting the level structure of Mg^{26}. However, the strong excitation of the 2^+ first excited state indicates that it has a collective nature. This is supported by the lifetime measurement of $(7\pm3)\times10^{-13}$ sec[53,55] which gives an $E2$ matrix strength, $|M(E2)|^2=12\pm5$ Weisskopf units.

It does not appear that there are any other strongly enhanced $L=2$ transitions, although the transition to the second excited state appears to have some enhancement. The excitation of the triplets centered at 4.33, 4.89, and 5.5 MeV is strong enough so that a 4^+ rotational level, formed by $L=4$, could conceivably be one of these 9 states. This is also true for a 3^-, $L=3$, vibrational level.

IV. COMPARISON OF THE (p,p') CROSS SECTIONS WITH E2 TRANSITION STRENGTHS

The results presented in the last section show that, as expected, there is a strong correlation between the larger (p,p') cross sections and the ground state EL transition strengths for a given nucleus. For the weakly excited levels the inelastic scattering measurements are often quite inaccurate so that meaningful comparisons are difficult to make. However, the few that can be made, and the observation of the (weak) excitation of levels for which excitation by a direct spin-independent interaction is forbidden, indicate that there is little or no correlation between $\sigma_T(p,p')$ and $|M(EL)|^2$ for weakly excited levels (or weak EL transitions).

The (p,p') cross section for the transfer of L units of angular momentum is expected to decrease rather rapidly with L other things being equal. The collective electric dipole states (i.e., the giant dipole resonance) are known to be at higher excitation energies than were accessible in the present work, so that $L=1$ transitions are not expected to be very large. On the other hand, the collective $E2$ states are known to be quite low in excitation—the first excited state, in fact, in even-even nuclei. Thus, it is not surprising that (p,p') cross sections for $L=2$ are found to be the largest observed. The (p,p') transitions proceeding via larger L values should be inhibited by the L dependence of the reaction mechanism and such seems to be the case. A few $L=3$ (p,p') transitions, which appear to be enhanced, can be identified. However, the vast majority which can be identified are $L=2$ (p,p') transitions and it is for these that we wish to compare in more detail the correlation between (p,p') cross sections and electromagnetic transition strengths.

Since there are only one or two strong $E2$ transitions known in each nucleus considered, the extent of the correlation between $\sigma_T(p,p')$ and $E2$ transition strengths can best be investigated by comparing the strong $E2$ transitions in different nuclei with one another. It is expected that the relation between $\sigma_T(p,p')$ and the

[55] V. K. Rasmussen, F. R. Metzger, and C. P. Swann, Phys. Rev. **123**, 1386 (1961).

$E2$ transition strength will be dependent upon the target nucleus, so that it is worthwhile to obtain some orientation by seeing what A dependence is predicted by the zero-range, spin-independent, plane-wave form of the direct-interaction (p,p') theory.

To this end, it is convenient to define the quantity,

$$R(E2)=\frac{(2J_0+1)}{(2J_1+1)}\frac{\sigma_T(p,p')}{\Lambda(E2)}, \tag{3}$$

where J_0 is the ground-state spin, $\sigma_T(p,p')$ is the total (p,p') cross section in mb for exciting the level with spin J_1, and $\Lambda(E2)$ is the $E2$ transition strength[56] which is related to $|M(E2)|^2$ for $r_0=1.2$ F by

$$\Lambda(E2)=0.61A^{4/3}|M(E2)|^2, \tag{4}$$

and to the radiative width by

$$\Gamma(E2)=8.02\times10^{-8}E_\gamma{}^5\Lambda(E2)\text{ eV} \tag{5}$$

where energies are in MeV and distances in Fermis.

Using the notation and definitions given by Warburton and Pinkston[57] for $\Lambda(E2)$ and for the zero-range, spin-independent, plane-wave Born approximation expression for $\sigma_T(p,p')$,[58] $R(E2)$ is given by

$$R(E2)=10\pi\Delta\left\{\int_0^\pi|\langle J_1\|\sum_{i=1}^{A}j_2(qr_i)Y_2(\Omega_i)\|J_0\rangle|^2\sin\theta d\theta\right\}\Big/|\langle J_0\|\sum_{i=1}^{A}r_i{}^2Y_2(\Omega_i)[1-\tau_3(i)]\|J_1\rangle|^2 \tag{6}$$

The quantity Δ is a slowly varying function of excitation energy (through k_f/k_i) and of A (through the reduced mass of the proton) and can be considered as constant for present purposes. The sum in the matrix element for $\sigma(\theta)$ is over all nucleons while the sum in the expression for $\Lambda(E2)$ is over the protons only. For the nuclei to be discussed, $A\approx2Z$, so that these sums should, to a good approximation, differ only by a constant. This is so because of the charge independence of nuclear forces. The r dependence in the two matrix elements of Eq. (6) can be separated out by defining suitable averages over the various oscillator shells contributing to the matrix elements. Then, if we define

$$F(r)=\left\{\int_0^\pi|\langle J_1\|j_2(qr)\|J_0\rangle_{\rm av}|^2\sin\theta d\theta\right\}\Big/|\langle J_0\|r^2\|J_1\rangle_{\rm av}|^2, \tag{7}$$

we have

$$R(E2)\propto F(r). \tag{8}$$

We are interested in the A dependence of $F(r)$. We note that, in general, the matrix element of $j_2(qr)$ will be a function of $b_pq(=x)$ where b_p is a nuclear distance. Since

$$q=k_i(1+\alpha^2-2\alpha\cos\theta)^{1/2}, \tag{9}$$

where α is defined as k_f/k_i, we can write, with $|\langle J_1\|j_2(qr)\|J_0\rangle_{\rm av}|^2=f(x)$,

$$\int_0^\pi f(x)\sin\theta d\theta=\frac{1}{b_p{}^2k_i{}^2\alpha}\int_{b_pk_i(1-\alpha)}^{b_pk_i(1+\alpha)}xf(x)dx. \tag{10}$$

For the plane wave case $f(x)$ decreases exponentially for large momentum transfers (see Appendix), and the upper limit in Eq. (10) can be replaced by ∞. Also, since $\alpha(=k_f/k_i)\approx1$ for the excitation of low-lying levels by protons with energies of 17 MeV or higher (for instance, $\alpha=0.8$ for excitation of a 6-MeV level by 17-MeV protons), and since the integrand goes to zero for $x\rightarrow0$, the lower limit to the integral can, to a good approximation, be replaced by 0. Thus, the integral on the right-hand side of Eq. (10) becomes independent of b_pk_i and α and

$$\int_0^\pi|\langle J_1\|j_2(qr)\|J_0\rangle_{\rm av}|^2\sin\theta d\theta\propto(b_p{}^2k_i{}^2\alpha)^{-1}. \tag{11}$$

On the other hand, it is well known that $|\langle J_0\|r^2\|J_1\rangle_{\rm av}|^2\propto b_e{}^4$ where b_e is a nuclear distance, not necessarily the same as b_p. Thus, we expect on the plane-wave theory that,

$$F(r)\propto(b_e{}^4b_p{}^2k_i{}^2\alpha)^{-1}. \tag{12}$$

As an example, $F(r)$ is derived in the Appendix for the special case that nucleons from only one oscillator shell contribute to the matrix elements of $j_2(qr)$ and r^2. The matrix elements are taken between harmonic oscillator wave functions for the two cases of the $1p$ and $1d$ shells using volume integration over all space as was used to obtain the solid curve of Fig. 1.

For the direct interaction model used here with the matrix element of $j_2(qr)$ evaluated using harmonic oscillator wave functions, a zero-range interaction and volume integration, the best fits are obtained with $b_p\approx R$ where $R=1.2A^{1/3}$ F. This is illustrated by the fit of Fig. 1, where the radial falloff distance used to give a best fit to the data was $b_p=2.6$ F while $1.2A^{1/3}=2.5$ F for Be^9. In the general distorted wave case it seems reasonable that b_p should be roughly proportional to the nuclear radius as well as approximately equal to it. Thus, we expect b_p to vary roughly as $A^{1/3}$.

The nuclear distance b_e used in evaluating the matrix element of r^2 is a different case. For harmonic oscillator wave functions it is usually assumed constant within a shell. However, high-energy (e,e') experiments[59] indicate

[56] A. M. Lane and L. A. Radicati, Proc. Phys. Soc. (London) **A67**, 167 (1954).

[57] E. K. Warburton and W. T. Pinkston, Phys. Rev. **118**, 733 (1959).

[58] $\sigma_T(p,p')=2\pi\int_0^\pi\sigma_\alpha(\theta)\sin\theta d\theta$ where the expression for $\sigma_\alpha(\theta)$ is given by Eq. (3a) of reference 57.

[59] H. F. Ehrenberg, R. Hofstadter, U. Meyer-Berkhout, P. G. Ravenhall, and S. E. Sobottkia, Phys. Rev. **113**, 666 (1959).

some A dependence for b_e also, and a variation of b_e^4 with A somewhere between $A^{1/3}$ and $A^{4/3}$ seems reasonable. Thus, for the plane-wave case we expect a variation of $F(r)$ with A from Eq. (12) somewhere between about A^{-1} and A^{-2}. The radial wave function of the nucleon making the transition has a radial dependence which is determined to a large extent by the binding energy of the nucleon as well as by the nuclear radius. Thus, b_p and b_e should also fluctuate with binding energy and thus from nucleus to nucleus. However, for the cases considered here the binding energies are quite large and this effect is not expected to be large compared to other uncertainties.

By their very nature, the collective transitions we are considering are expected to contain contributions from many oscillator shells, and as shown in the Appendis, $F(r)$ is dependent on the relative weights of the various oscillator shells contributing to the transition. Thus, in addition to the A dependence implied by Eq. (12), we should not be surprised by sharp changes in $R(E2)$ which can come about because of variations in the relative weights of the oscillator shells from transition to transition. In particular, there is the possibility of a discontinuity in $R(E2)$ as the $1p$ shell is closed at O^{16}. This possibility is illustrated in the Appendix.

We are now ready to compare the stronger (p,p') cross sections obtained at this laboratory with ground state $E2$ transition strengths. Table IX summarizes the data used in this comparison. The transition strength for the Li^6 transition is a theoretical value calculated from Eq. (12) of Warburton and Pinkston[57] with a factor inserted to take account of the core

TABLE IX. Ground state $E2$ transition strengths, $\Lambda(E2)$, and total (p,p') cross sections, $\sigma_T(p,p')$, for some low-lying levels in light nuclei.

Nucleus	J_0	J_1	E_x (MeV)	$\Lambda(E2)$[a]	E_p(c.m.) (MeV)	$\sigma_T(p,p')$	References
Li^6	1^+	3^+	2.18	22(theo.)	16.7	58±10	b, c
Be^9	$3/2^-$	$5/2^-$	2.43	···	17.0	67±6	···
B^{10}	3^+	1^+	0.72	42±1	16.3	8.4±2	d
C^{12}	0^+	2^+	4.43	81±12	16–18	130±5	e, f
O^{16}	0^+	2^+	6.92	44±11	17.9	17±10	e, g
Ne^{20}	0^+	2^+	1.63	1060_{-360}^{+200}	16.6	91±9	e, h
Mg^{24}	0^+	2^+	1.37	1100±250	17.3	117±12	i, j
Mg^{25}	$5/2^+$	$7/2^+$	1.61	850±210	16.7	41±6	k
Mg^{26}	0^+	2^+	1.83	570±170	17.4	61±6	k, l
Fe^{56}	0^+	2^+	0.85	1780±400	17.0	40±5	m, n, o
Ni^{58}	0^+	2^+	1.45	2220±550	16.5	50±4	m, p

[a] For $r_0=1.2$ F, $\Lambda(E2)=0.61A^{4/3}|M(E2)|^2$.
[b] Theoretical value for $\Lambda(E2)$, see text.
[c] Reference 2.
[d] Reference 41.
[e] Reference 25.
[f] Reference 3.
[g] Reference 5.
[h] Reference 45.
[i] S. Ofer and A. Schwarzschild, Phys. Rev. Letters **3**, 384 (1959).
[j] Reference 6.
[k] Reference 53.
[l] Reference 55.
[m] D. G. Alkazov, A. P. Grinberg, K. I. Erokhina, and I. Kh. Lemberg, Izvest. Akad. Nauk. S. S. S. R., Ser. Fiz. **23**, 223 (1959).
[n] G. M. Temmer and N. P. Heydenburg, Phys. Rev. **104**, 967 (1956).
[o] P. C. Gugelot and P. R. Phillips, Phys. Rev. **101**, 1614 (1956).
[p] W. W. Daehnick and H. A. Hill (unpublished).

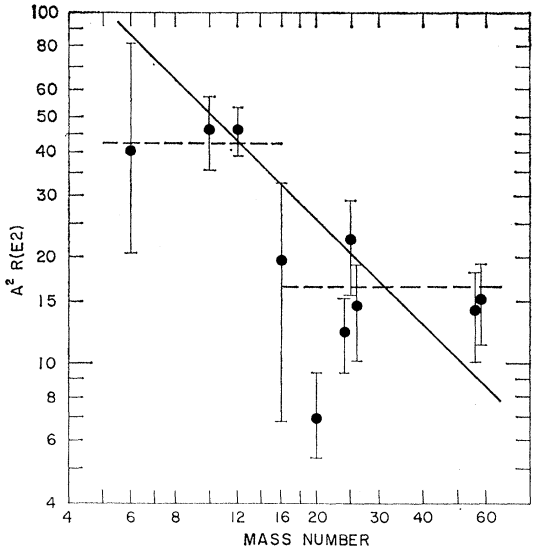

FIG. 19. Comparison of the total (p,p') cross section $\sigma_T(p,p')$, with the electric quadrupole transition strength, $\Lambda(E2)$, for some low-energy $E2$ ground-state transitions in light $(6\leq A<60)$ nuclei. The factor $A^2R(E2)=A^2[(2J_0+1)/(2J_1+1)][\sigma_T(p,p')/\Lambda(E2)]$ is shown plotted against A. The error bars are due to the experimental uncertainties in $\sigma_T(p,p')$ and $\Lambda(E2)$. The solid line has a slope of A^{-1}. The dashed horizontal lines are explained in the text.

motion. The result was $\Lambda(E2)=11$ for the LS limit. The result was quite insensitive to reasonable departures from the LS extreme. A collective enhancement of a factor of 2 and an uncertainty of the same amount was arbitrarily assumed for this transition strength. The other transition strengths are published experimental values. The $\sigma_T(p,p')$ which are not taken from the present work were obtained by integrating (p,p') angular distribution curves all of which were obtained at this laboratory.

In Fig. 19, $A^2R(E2)$ obtained from Table IX from the relation

$$R(E2)=\frac{2J_0+1}{(2J_1+1)}\frac{\sigma_T(p,p')}{\Lambda(E2)},$$

is shown plotted against A. The factor A^2 is inserted mainly to straighten the slope of the trend of the points; but also because A^{-2} is the strongest A dependence predicted by the plane-wave theory. It is clear that there is a strong correlation between $\sigma_T(p,p')$ and $\Lambda(E2)$. Except for the Ne^{20} transition, all the points lie within a factor of 2 of a straight line through the points. The solid straight line shown in the log-log plot of Fig. 19 has a slope of A^{-1} and thus is for an A^{-3} dependence for $F(r)$. The two horizontal dashed lines are drawn on the assumption that $F(r)$ has an A^{-2} dependence and has a discontinuity of 2.6 at O^{16}. This "shell effect" is predicted by one form of the plane-wave direct interaction model with the severe restriction that only $1p\rightarrow 1p$ transitions take place for p-shell nuclei and only $1d\rightarrow 1d$ transitions for nuclei above O^{16} (see the Appendix).

The scatter of the points in Fig. 19 and the errors associated with these points are too large to allow a choice between the two forms of the $A^2R(E2)$ vs A curve shown. However, a comparison of Fig. 19 with the predictions of the plane wave theory does give some information concerning the A dependence of the effects of distortion on $R(E2)$. From Fig. 19 it is clear that $R(E2)$ has a smoothed-out A dependence which can roughly be characterized by A^{-n} with n a positive number. If there is no "shell effect" then $n\approx 3$ and in this case it seems that distortion introduces an A dependence of $n\approx 1$ to 2 in $R(E2)$ in addition to that given by the plane wave theory. If there is a "shell effect" of the amount indicated in Fig. 19 then distortion would seem to introduce an additional A dependence of $n\simeq 0$ to 1. In any case, then, the effect of the distortion on $R(E2)$ can be roughly characterized by A^{-n} with $n\simeq 0$ to 2.

Nine out of ten of the points in Fig. 19 lie within 40% of the dashed lines, thus, given the (p,p') cross section of a strong $L=2$ transition for $6\leq A<60$ at $E_p=17$ MeV the present result would indicate that we can predict $\Lambda(E2)$ to 40% with something like 90% confidence. As an example, consider the Be^9 2.43-MeV level. Using $A^2R(E2)=42.5$ (the dashed curve of Fig. 19) and the $\sigma_T(p,p')$ given in Table IX, we get $\Lambda(E2)=85$, or $|M(E2)|^2=7.5$ for this transition.

It is of interest to compare the present results with the (p,p') experiments performed at $E_p=180$ to 140 MeV.[17,60] The effects of distortion are presumably considerably less at these energies so that such a comparison should give us some idea of the effects of distortion on the correlation between $\sigma_T(p,p')$ and $\Lambda(E2)$. Tyrén and Maris[17] obtained (p,p') angular distributions for C^{12} and Be^9 at 185 MeV. Evaluating $A^2R(E2)$ from their data on the C^{12} 4.43-MeV level, and using their data for the Be^9 2.43-MeV level leads to $\Lambda(E2)\simeq 105$, or $|M(E2)|^2\simeq 9.0$, for the latter state in satisfactory agreement with our result. Clegg *et al.* used about 140-MeV protons in a study of $(p,p'\gamma)$ cross sections in various p-shell nuclei. Their results for B^{10} and C^{12} can be compared to ours. In an analysis similar to the one given here, they find an $E2$ radiative width of 9.7×10^{-4} eV for the B^{10} $2.15\rightarrow 0$ transition, this width corresponds to $|M(E2)|^2=20$ with an uncertainty of about 35% from the cross-section measurements alone, while the present results (see Sec. III B) give $|M(E2)|^2=1\pm 0.35$. The large discrepancy is difficult to understand. A lifetime measurement of the B^{10} 2.15-MeV level would help to resolve this disagreement. If the discrepancy is real, i.e., not due to experimental difficulties, then the conclusion is inescapable that distortion is destroying the correspondence between $\sigma_T(p,p')$ and $\Lambda(E2)$ at $E_p=17$ MeV for this transition.

[60] A. B. Clegg, K. J. Foley, G. L. Salmon, and R. E. Segel, Proc. Phys. Soc. (London) **78**, 681 (1961).

V. SUMMARY AND CONCLUSIONS

The major points of the (p,p') results at $E_p=17$ MeV can be summarized as follows:

1. The angular distributions show the forward peaking characteristic of a direct interaction. However, the peaking is sharper than predicted by the plane-wave theory. This fact, together with an observed lack of sharp maxima and minima, is ascribed to initial and final state interactions.

2. For each nucleus the larger (p,p') cross sections for the different excited states are in good qualitative agreement with (α,α') and (d,d') results. This agreement indicates that the spin-dependent interaction does not play a major role in exciting these states. However, for (α,α') and (p,p') there is weak excitation of states which cannot be excited by a spin-independent direct interaction. This shows that—at most—only a slight correlation should be expected between $\sigma_T(p,p')$ and $\Lambda(EL)$ for weakly excited levels.

3. For each nucleus the larger (p,p') total cross sections show a proportionality with the $\Lambda(EL)$. This is most noticeable in Mg^{25} and Be^9. In particular, the Mg^{25} results support the rotational model proposed for that nucleus. The Be^9 results also support a rotational model interpretation of that nucleus. In B^{10} the strongest transition is to a state (or states) at 6.04 ± 0.05 MeV. This state is probably the 4^+, B^{10} 6.04-MeV level. It has been suggested by Blair[61] that this 4^+ state is a higher rotational state of the ground-state configuration Thus, the present results give additional support to the discussion of Clegg[62] that the $1p$ shell is amenable to a rotational model interpretation and that inelastic scattering is a natural tool for investigating this rotational character.

4. A strong correlation was found between $\sigma_T(p,p')$ and $\Lambda(E2)$ for the stronger (p,p') transitions (Fig. 19) leading to the lowest collective $E2$ state of those nuclei studied in this laboratory. This correlation was compared to the crude assumption of a plane-wave, zero-range, spin-independent direct interaction in order to obtain some orientation to its A dependence. The comparison showed that the effects of distortion on the ratio $R(E2)$ defined in Sec. IV has a smoothed-out A dependence which can be characterized by A^{-n} with $n\simeq 0$ to 2. The possibility of a "shell effect" in $R(E2)$ was discussed. The data for $\Lambda(E2)$ were not good enough to decide whether or not such an effect exists.

5. The ratio $R(E2)$ for the Ne^{20} first excited state appears about a factor of 2 to 3 lower than expected from the other data. In other words, $\sigma_T(p,p')$ for this level is smaller than expected from the large $\Lambda(E2)$ measured for the ground-state transition from this level. It would be interesting to obtain $\sigma_T(p,p')$ for the O^{18} first excited state and the F^{19} second excited state to see whether there is a generally low value of $R(E2)$ near $A=20$.

[61] J. S. Blair (private communication).
[62] A. B. Clegg, Phil. Mag. **6**, 1207 (1961).

ACKNOWLEDGMENTS

We would like to thank J. Christenson and H. L. Berk for their assistance in analyzing the data. One of us (E. K. W.) is indebted to K. J. Foley for discussions concerning the Oxford (p,p') experiments at a proton energy of 140 MeV.

APPENDIX

In this Appendix we derive the factor $F(r)$ given in Eq. (7) for the special case that only nucleons from one oscillator shell contribute to the matrix elements of $j_2(qr)$ and r^2. We consider the $1p$ and $1d$ shells and evaluate the matrix elements by integrating over all space, using harmonic oscillator wave functions. This is the method often used[56,57] to evaluate the radial integrals of r^2 and is the method used by Levinson and Banerjee to evaluate the radial integral of $j_2(qr)$ in the plane-wave Born approximation for the (p,p') cross section. The results of this volume integration are

$$\begin{aligned}
|\langle j_2(qr)\rangle_{1p}|^2&=(y^2/36)e^{-y/2},\\
|\langle j_2(qr)\rangle_{1d}|^2&=(y^2/3600)(14-y)^2e^{-y/2},\\
|\langle r^2\rangle_{1p}|^2&=(25/4)b_e^4,
\end{aligned}\tag{A1}$$

and

$$|\langle r^2\rangle_{1d}|^2=(49/4)b_e^4,$$

where $y=(b_pq)^2$ and b_p and b_e are the radial falloff distances of the harmonic oscillator wave functions, not necessarily the same in the matrix elements, of $j_2(qr)$ and r^2. We need to evaluate the integrals,

$$\int_0^\pi (y^2/36)e^{-y/2}\sin\theta d\theta$$

and

$$\int_0^\pi (y^2/3600)(14-y)^2e^{-y/2}\sin\theta d\theta.\tag{A2}$$

Both integrals have terms which can be put into the form,

$$\int_0^\pi y^ne^{-y/2}\sin\theta d\theta=\frac{-1}{2a\alpha}\int_{a(1+\alpha)2}^{a(1-\alpha)2} y^ne^{-y/2}dy\tag{A3}$$

where $a=b_p^2k_i^2$, $\alpha=k_f/k_i$, and $y=a[1+\alpha^2-2\alpha\cos\theta]=b_p^2q^2$. Writing $I_n(y)=-\int y^ne^{-y/2}dy$, we have for $n=2$,

$$I_2(y)=-2(8+4y+y^2)e^{-y/2}.\tag{A4}$$

Since $k_i=0.9$ F^{-1} for 17-MeV protons and $\alpha(=k_f/k_i)$ is larger than 0.8 for excitation energies less than 6 MeV for 17-MeV protons, the lower limit, $b_p^2k_i^2(1+\alpha)^2$, on the integral on the right-hand side of Eq. (A3) is greater than 16 for the cases to be considered, so that the $e^{-y/2}$ factor causes the contribution from the lower limit to be negligibly small. The upper limit is such that $I_2(a(1-\alpha)^2)\cong I_2(0)$ so that $I_2(y)=-16$ to a very good approximation. The same arguments hold for all the $I_n(y)$ with the result that

$$\int_0^\pi y^ne^{-y/2}\sin\theta d\theta=\frac{(n!)2^n}{a\alpha};\tag{A5}$$

thus

$$\begin{aligned}
F(r)_{1p}&=(8/225)(b_e^4b_p^2k_i^2\alpha)^{-1},\\
F(r)_{1d}&=(3.1/225)(b_e^4b_p^2k_i^2\alpha)^{-1}.
\end{aligned}\tag{A6}$$

Since these $F(r)$ differ by a factor of 2.6, a decrease in $R(E2)$ of this amount or more at O^{16} is predicted by the model used if the contribution to the $E2$ transition were all from the $1p$ oscillator shell for p-shell nuclei and all from the $1d$ oscillator shell for $(2s,1d)$-shell nuclei. The discontinuity could be more than a factor of 2.6 because both b_e and b_p might increase sharply between the p-shell nuclei and the (s,d)-shell nuclei. However, it is expected that a large number of oscillator shells contribute to collective $E2$ transitions. For instance, Rost[16] found that about 40% of the $E2$ transition between the first excited state and the ground state of Mg^{24} was due to $1d\rightarrow 1d$ transitions, the rest being due to transitions from the $1p$ and $1d$ shells to higher shells. In this case $|\langle j_2(qr)\rangle|^2$ and $|\langle r^2\rangle|^2$ would be averages over the oscillator shells contributing to the transition and the "shell effect" might be smoothed out to a negligible effect. Thus, the present considerations illustrate how a "shell effect" in $R(E2)$ can come about but do not demand such an effect even for the form of the direct-interaction model which is assumed.